



# Review of Soft Actuator Materials

Jaehwan Kim<sup>1</sup> · Jung Woong Kim<sup>1</sup> · Hyun Chan Kim<sup>1</sup> · Lindong Zhai<sup>1</sup> · Hyun-U Ko<sup>1</sup> · Ruth M. Muthoka<sup>1</sup>

Received: 25 March 2019 / Revised: 2 October 2019 / Accepted: 6 October 2019 / Published online: 18 October 2019  
© Korean Society for Precision Engineering 2019

## Abstract

Soft actuator materials change their shape or size in response to stimuli like electricity, heat, light, chemical or pH. These actuator materials are compliant and well suited for soft mechatronics and robots. This paper introduces the definition of soft materials and the position of soft actuator materials in comparison with conventional actuators and other solid state actuator materials. A thorough review of selected soft actuator materials is carried out, including responsive gels/hydrogels, ionic polymer metal composites, conducting polymers, carbon nanotubes/graphenes, dielectric elastomers, shape memory polymers and biopolymers. This review will give insights for applications of soft actuator materials via better understanding of the materials in terms of their preparation, performance and limitation.

**Keywords** Soft actuators · Smart materials · Electroactive polymers · Responsive gels · Shape memory polymers

## 1 Introduction

Actuator is one of fundamental and important technologies that produce motion for many industrial applications including robotics, automobiles, military facilities and consumer products. Traditionally, pneumatic, hydraulic and electromagnetic technologies have been used for actuators. These traditional actuator technologies exhibit good energy efficiency but low work and power densities since they are made with hard and heavy materials. Modern technologies are evolved by the motto of ‘smaller, lighter, faster and softer.’ The smaller and

lighter robots consume less energy so as to reduce the weight and can move faster. Softer robots, composed of compliant materials similar to those found in living organisms, can allow for increased flexibility and adaptability for accomplishing tasks, as well as improved safety.

The next generation of actuators for soft robots that will surpass the state-of-the-art challenges requires a bold departure from the traditional actuator technologies while clearly counting on the valuable research accomplishments to date. In late 1990s, the concept of smart materials has been introduced [1]. Smart material system is a non-biological physical material system having the following attributes: a definite purpose, means and imperative to achieve that purpose and a biological pattern of functioning. In smart material system, actuator materials have the ability to change the shape, stiffness, position, natural frequency, damping and/or other mechanical characteristics of the smart material systems in response to changes in temperature, electric field and/or magnetic field. These actuator materials belong to a solid state actuator technology that has high energy density and power density. Table 1 shows solid state actuator technologies in comparison with traditional ones and muscles. There are several solid state actuator materials including shape memory alloy (SMA), piezoelectric, magnetostrictive, electrostrictive and electroactive polymer (EAP). Mostly, traditional actuator technologies possess high efficiency meanwhile solid state actuator technologies exhibit high work or power density.

---

This paper is an invited paper.

---

✉ Jaehwan Kim  
jaehwan@inha.ac.kr

Jung Woong Kim  
jw6294@naver.com

Hyun Chan Kim  
Kim\_HyunChan@naver.com

Lindong Zhai  
duicaofei@naver.com

Hyun-U Ko  
lostmago@naver.com

Ruth M. Muthoka  
mwongelinruth@gmail.com

<sup>1</sup> Department of Mechanical Engineering, CRC for Nanocellulose Future Composites, Inha University, Incheon 22212, Korea

**Table 1** Comparison of solid state and traditional actuator technologies

| Actuator technology    | Material             | Max. stress (MPa) | Max. strain (%) | Efficiency (%) | Bandwidth (Hz) | Work density (J/cm <sup>3</sup> ) | Power density (W/cm <sup>3</sup> ) |  |
|------------------------|----------------------|-------------------|-----------------|----------------|----------------|-----------------------------------|------------------------------------|--|
| Traditional [2]        | Electromagnetic      | 0.02              | 50              | 90             | 20             | 0.005                             | 0.1                                |  |
|                        | Hydraulic            | 20                | 50              | 80             | 4              | 5                                 | 20                                 |  |
|                        | Pneumatic            | 0.7               | 50              | 90             | 20             | 0.175                             | 3.5                                |  |
| Muscle [3]             | Fruit fly            | 0.04              | 1               | 10             | 200            |                                   |                                    |  |
|                        | Cockroach            | 0.174             | 12              |                |                |                                   |                                    |  |
|                        | Biological           | 0.35              | 20              | 30             | 10             | 0.035                             | 0.35                               |  |
| Solid state            | SMA [2]              | 200               | 10              | 3              | 6              | 10                                | 30                                 |  |
|                        | Piezoelectric [2]    | 35                | 0.2             | 50             | 5000           | 0.035                             | 175                                |  |
|                        | Electrostrictive [2] | 50                | 0.2             | 50             | 5000           | 0.050                             | 250                                |  |
|                        | Magnetostrictive [2] | 35                | 0.2             | 80             | 2000           | 0.035                             | 70                                 |  |
|                        | <i>EAP</i>           |                   |                 |                |                |                                   |                                    |  |
|                        | Dielectric elast [4] | 0.6               | 215             |                | 60–80          | ~ kHz                             |                                    |  |
|                        | IPMC [5]             | 2                 | 0.3             |                |                |                                   |                                    |  |
|                        | Twisted CNT yarn [6] | 200               | 1               |                |                |                                   |                                    |  |
| Conducting polymer [7] | 34                   | 6                 |                 | 2              | 2              |                                   |                                    |  |

In last three decades, the field of EAP has received much attention as a result of the development of new EAP materials that exhibit a large deformation. This characteristic is a valuable attribute that has enabled a myriad of potential applications, and it has evolved to offer operational similarity to biological muscles. EAPs, in other words soft actuators, are able to offer a range of performance and soft characteristics that may not be reproduced by other technologies. Owing to light-weight, flexible and high energy efficiency, soft actuators allow the researchers the opportunity to design compact, light-weight and compliant actuators to be used in autonomous soft robots. Soft robots consisting of soft and flexible materials without rigid components have attracted tremendous interest because of their potential to improve the capabilities of traditional hard robotic systems [8]. The compliant property of the soft materials allows the structure to deform according to its surroundings. As a result, it is capable of absorbing energy during impact, interacting with humans, manipulating fragile items, and traversing through rough and unpredictable terrains [9–11]. Soft nature of the materials also provides higher degrees-of-freedom motions without needing any joints or hinges.

Reviews of current developments in soft actuators have been recently reported including the performance comparison and application-specific selection criteria [12–15]. A special importance is given to seven selection criteria, including the aspect of compliance, topology-geometry, scalability, energy efficiency, operation range, modality, controllability and technological readiness level. Biomimetic robots have been demonstrated by utilizing soft actuator materials for underwater robots, insect-inspired

robots, flapping robots and wheel robot [16–20]. Additive manufacturing, for example, 3D printing, has been popular for various products fabrication because of its free-form manufacturing ability. Advances in soft materials and additive manufacturing technologies have enabled the design of soft robots with sophisticated capabilities, such as jumping, complex 3D movements, gripping and releasing [21–27]. Advantages and limitations of different additive manufacturing processes, including 3D printing, fused deposition modelling, direct ink writing, selective laser sintering, inkjet printing and stereolithography, were discussed, and the different techniques were investigated for their application in soft robotic fabrication [28, 29].

This paper reviews all about soft actuator materials. Soft actuators belong to EAPs made with soft materials. Soft materials are easily deformable materials that include liquids, polymers, foams, gels, colloids, granular materials and etc. Over recent years, intensive efforts have been devoted to the development of soft materials that possess extraordinary mechanical properties, especially by seeking inspiration from nature and biology. A question is that how we can distinguish soft from hard in EAP or solid state actuator materials. In other word, where is boarder line that distinguishes hard and soft actuator materials. To understand this issue, elastic moduli of solid state actuator materials are drawn in Fig. 1 in comparison with human organs. It is obvious that most human organs are soft except bones and enamels. In solid state actuator materials, hydrogels, gels, dielectric elastomers (DEs), ionic polymer metal composites (IPMCs), PVDF (a piezoelectric polymer) and up to polypyrrole (PPy) can be categorized into soft materials. On the other hand,

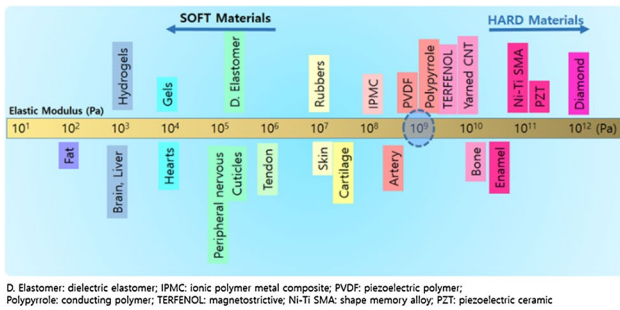


**Fig. 1** Elastic modulus comparison of soft materials in comparison with human organs

PZT (a piezoelectric ceramic), Ni–Ti SMA and TERFENOL (a magnetostrictive) are known to be hard materials due to their solid state. However, elastic modulus of the yarned carbon nanotube (CNT), known as EAP, is higher than that of TERFENOL. This means that high elastic modulus of the yarned CNT along with its flexible behavior is beneficial for producing high mechanical work. Nevertheless, the rule of thumb that distinguishes soft actuator materials can be made with elastic modulus in the range of GPa.

Note that soft actuators can be made not only by soft actuator materials but also with novel mechanisms incorporating air pressure, origami structure, biomimetic structures and hybrid composites. For example, SMA wires reinforced polymer composites can be controlled their shapes by heating and cooling the wires with electric current. In fact, one of the most widely used mechanisms for controlling these soft materials is by using pneumatic actuation, where air is pumped into individual cells to locally inflate the structure and induce motion. However, techniques that involve fluid pressure require tethered tubes and external compressors, which can cause the system to become bulky and heavy. Thus, this paper only covers soft actuator materials including gels/hydrogels, IPMCs, conducting polymers (CPs), CNTs and graphene, DEs, shape memory polymers (SMPs) and biopolymers. Recent advances of soft actuator materials are reviewed. This review will give insights for applications of soft actuator materials via better understanding of the materials in terms of their preparation, performance and limitation.

## 2 Gels and Hydrogels

Gel is a solution or colloidal suspension that undergoes a physical or chemical change to a solid while retaining much of solvent within the structure. According to recent definition, a gel is an elastic solid material composed of at least two components, one of which polymer forms a physically or chemically bonded three-dimensional network that occurs

in a medium of another component, a liquid, wherein the amount of the liquid is sufficient for ensuring the elastic properties of the gel [29]. It consists of an elastic cross-linked network and a fluid filling the interstitial spaces of the network [30]. The network of long polymer molecules holds the liquid in place to give the gel solidity. Gels take many forms, including copolymers, blends, or interpenetrating networks. Figure 2 shows schematics of gels and hydrogels. Gels are wet and soft and look like solid material but are capable of undergoing large deformation in response to environmental change. It shows a yield strength and a measurable elastic modulus, at which the yield strength is sufficiently low so that the gel may be considered as a structural liquid. Gels can be categorized into physical and chemical gels depending on their crosslink network. Figure 3 shows the family of gels. Physical gels are formed by physical crosslinks which are reversible from liquid-like to solid-like behavior. They are characterized by the presence of one or two yield points at stresses above which network degradation and gel transition from the solid to the fluid state take place. Examples of physical gels are gelatin, agarose and clays. Chemical gels are formed by chemical crosslinks like covalent bonds, which are irreversible. Almost any water-soluble polymer can be prepared as gel by carrying out the polymerization in the presence of cross linking agent or by carrying out a cross-linking reaction on a solution of the polymer [3]. Polyacrylamide, polyacrylic acid,

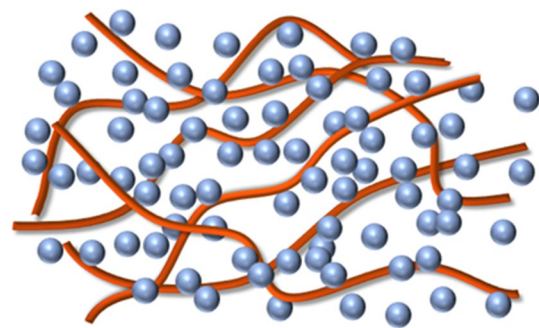


**Fig. 2** Schematics of gels and hydrogels consist of immobile network and mobile solvent

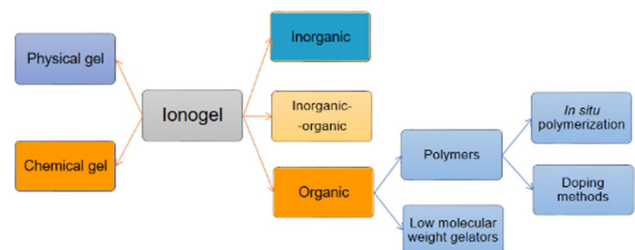


**Fig. 3** The classification of gels/hydrogels

hydroxy-ethylmethacrylate, silicon and vinylpyrrolidone are known to be chemical gels.

Hydrogels are three dimensional network structures consisting of polymeric chains joined by tie points or joints and swollen in water up to thermodynamic equilibrium [31]. They are hydrophilic polymers crosslinked into an insoluble, but highly hydrophilic structure, at which networks are formed by covalent bonds, ionic bonds, hydrogen bonds, physical entanglements or dipolar interactions. Hydrogels possess numerous properties that make them ideal candidates for use as biomaterials, finding significant use in the fields of drug delivery, tissue engineering, implants, and more. Their hydrophilic and crosslinked nature also imparts excellent biocompatibility, and many common hydrogels have found wide use both in laboratory studies and clinical uses. Some of the most commonly used hydrogels include synthetics like poly(ethylene glycol) (PEG), poly(vinyl alcohol) (PVA), or poly(2-hydroxyethyl methacrylate), as well as naturally occurring hydrogels like agarose, alginate, cellulose, chitosan, collagen, fibrin, and hyaluronan [32–34]. Hydrogels become especially useful when they are used as actuator materials that can respond to changes in their environment. In this review, we discuss multiple responsive modalities—including responses to pH, temperature, chemicals, light and electric fields.

Organogels are gels composed of an organic liquid phase which is immobilized by a crosslinked three-dimensional network [35]. Despite their majority is liquid composition, these systems demonstrate the appearance and rheological behavior of solids. They are attractive for drug delivery platforms for active agent administration via diverse routes such as transdermal, oral, and parenteral. Polyelectrolyte gels are made with ionizable polymers including anionic polymers such as the salts of polyacrylic acid, polymethacrylic acid and polystyrenesulfonic acid [30]. There is a family of cationic polymers, which share the acid–base characteristics of the equivalent salts. Depending upon the ionization levels, they are activated in the presence of pH change and temperature change. A special class of polyelectrolyte gels is ionic gel or ionogel. Ionogel is a gel where an ionic liquid (IL) is immobilized within a crosslinked network. Ionogels combine the physical properties of both the polymer and the physically entrapped IL keeping the main properties of IL, for example, ionic conductivity, non-volatility, non-flammability, except outflow and the mechanical stability of the host network [36]. IL is an organic salt with melting temperature below 100 °C. When the melting temperature is lower than 20 °C, they are called room temperature ionic liquids. ILs have interesting properties such as nonvolatility, high stability, suitable polarity, high ionic conductivity, and easy recyclability. Owing their ideal properties, ILs are receiving much attention as environmentally benign solvents for organic chemical reactions, separations, and

for electrochemical applications. Recent developments involve their use for biopolymers, molecular self-assembly, electrochemical machining, smart materials and actuators [25, 37–40]. Ionogels are considered as hybrid materials, in which the properties of IL are hybridized with those of another component [41]. These novel hybrid materials are indicated for possible applications as catalytic, separation, or ion conducting membranes. There are two main approaches to the immobilization of IL. ILs are immobilized by chemical attachment of ionic species to a solid support, or by the physical fixation of IL without covalent linkage within a host network. Comparing with hydrogels or organogels, ionogels show high mechanical strength, tunable elastic response and rapid recovery ability after the deformation [36].

Stimuli-responsive gels represent a broad class of gels undergoing switchable gel-to-solution or gel-to-solid transitions upon application of external stimuli [42]. Different physical or chemical external stimuli can be applied to induce reversible or single-cycle phase transitions of the hydrogels. These include thermal, magnetic, ultrasonic, electrochemical, or light stimuli as physical triggers, and pH, redox reactions, supra-molecular complexes, and biocatalytically driven reactions as chemical triggers. Numerous applications of stimuli-responsive hydrogels include their use as functional matrices for sensing, actuators, and biomedical applications, such as controlled drug release, tissue engineering, and imaging [31, 43]. Some of important stimuli responsive gels are briefly explained.

## 2.1 pH Responsive

pH-responsive hydrogels are a subset of stimuli-responsive hydrogels that have pH-induced deswelling/swelling behavior [31]. These pH-responsive hydrogels are of particular interest for biomedical applications as several locations in the body exhibit substantial pH changes associated with normal function or as part of a disease state. The pH responsive behavior of the hydrogel network is imparted by the presence of ionizable pendant groups in the polymer backbone. Two different families of pH-responsive hydrogels exist that differ in their pendant group ionization and subsequent swelling behavior. The generation of electrostatic repulsive forces results in the pH dependent swelling and deswelling processes as the water is either absorbed or expelled from the hydrogel network. Anionic hydrogel networks contain pendant groups that are ionized in solutions at a pH greater than their acid dissociation constant,  $pK_a$ , which swells because of the large osmotic pressure generated by the presence of the ions. Conversely, cationic pendant groups are ionized at a pH less than their  $pK_a$  and the corresponding hydrogel network is, therefore, swollen. Figure 4 shows these swelling behaviors [31]. Anionic hydrogel networks remain collapsed at low pH due to the presence of physical interactions (i.e.

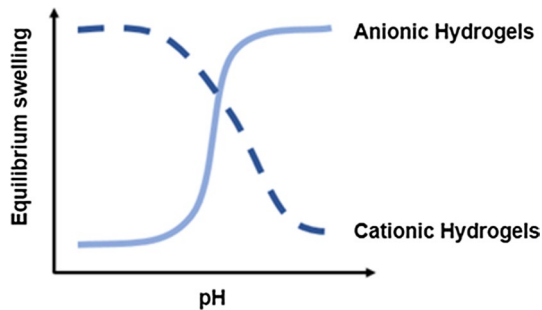


**Fig. 4** Equilibrium swelling behaviors of anionic and cationic hydrogels [31]

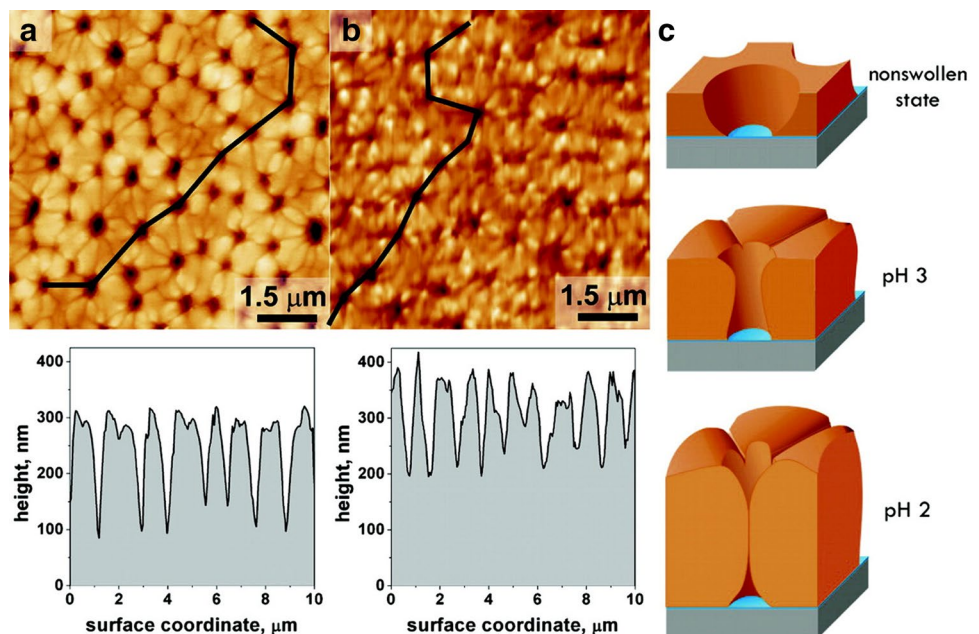
hydrogen bonding) that keep the network tightly complexed. Once the pH increases above the  $pK_a$  of the polymer, the complexes dissociate due to changes in the ionic character and the polymer swells due to a combination of electrostatic repulsion and water imbibition. The most common anionic monomers used to introduce pH-responsive behavior include acrylic acid, methacrylic acid. Cationic hydrogel networks exhibit opposite swelling behavior to anionic hydrogels. The swelling behavior is triggered by a decrease in the pH of the surrounding area. Dimethylaminoethyl methacrylate, diethyl-aminoethyl methacrylate and acrylamide (AAm) are known to be common cationic monomers for pH-responsive hydrogels.

In order to control flow and permeability of membranes ultrathin hydrogel membranes, Poly(2-vinylpyridine) (P2VP) was chemically crosslinked by 1,4-diodobutane, which exhibited that the pore size and therefore permeability can be controlled by the expansion or shrinkage of the

network upon pH changes, which regulate the pore “open” or “close” operations [43]. Such reversible pore size changes provide good controllability in fabricating flow gate membranes. Figure 5 shows the surface images of the crosslinked P2VP hydrogels with different pH levels [44].

Natural polymers such as albumin, gelatin, alginate and chitosan can also exhibit pH-responsive behavior [31]. Polysaccharides such as chitosan, cellulose and alginate undergo physical crosslinking due to hydrophobic or charge interactions. Swelling occurs as a result of the ionization of groups along the polysaccharide chain resulting in the buildup of charge and subsequent electrostatic repulsion and swelling. Water-soluble cellulose derivatives can be used to form hydrogel networks possessing specific properties in terms of swelling capability and sensitivity to external stimuli [45]. The smart behavior of some cellulose derivatives for example, hydroxypropyl methylcellulose, sodium carboxymethylcellulose, in response to pH and temperature variations, makes the resulting hydrogels particularly appealing for soft actuator applications. Natural pH-responsive polymers are biocompatible and biodegradable materials which are promising especially for in cases where environmental issues are concerned, as well as biomedical applications [46]. A pH-responsive hydrogel with improved mechanical and dielectric properties from cellulose nanocrystals (CNCs) exhibited a pronounced change in their swelling index in response to variation in pH [47, 48]. At low pH, the  $CNC-NH_2$  gel formed aqueous dispersions in water on account of electrostatic repulsions of the ammonium moieties inhibiting aggregation. However, a transition to hydrogel was observed at higher pH where the  $CNC-NH_2$  gel was neutral and the attractive forces based on hydrogen bonding dominated.

**Fig. 5** SPM topography images of crosslinked P2VP hydrogels at **a** pH 2 and **b** pH 3. **c** Schematic representation of cross-section profiles of the pore in the shrinkage and expansion states [44]



The opposite behavior was observed for the CNC–CO<sub>2</sub>H gel, which was dispersible at high pH.

## 2.2 Temperature Responsive

Temperature responsive hydrogels fall into two primary categories, positively and negatively responsive systems. Normally, these systems are identified by having an upper critical solution temperature (UCST) or a lower critical solution temperature (LCST), respectively. The expansion or collapse that correlates with the critical shift in aqueous solubility has been utilized as a mechanism for actuation and in situ gelling scaffolds for tissue regeneration [31]. The swelling response of reverse thermo responsive gels, the LCST response has been studied for poly(*N*-isopropylacrylamide) (PNIPAAm) and other alkyl-substituted acrylamides. The primary limitations, however, are the slow responsive rates and relatively weak mechanical integrity of the networks. To improve these properties PNIPAAm was copolymerized with acrylic acid, interpenetrated with poly(methacrylic acid), or grafted with hydrophilic/hydrophobic pendant chains to form comb-like systems [43]. Rapid-responsive kinetics and enhanced gel stabilities can be achieved in these systems by utilizing capillary froths, interchain hydrogen bonding interactions and formation of water release channels. Although UCST systems are less common than LCST, the common UCST hydrogel is an inter-penetrating network composed of interlocking networks of acrylic amide and acrylic acid. Cellulose microfibrils physically bound together by soft hemicellulose chains form the scaffolding that makes plant cell walls strong. Inspired by this architecture, biomimetic temperature responsive hydrogel networks have been reported by reinforcing CNC and methylcellulose (MC) [49]. Figure 6 shows the schematic of cellulose nanocomposite hydrogel and its thermo-responsive behavior under cooling and heating. At 20 °C, the storage modulus was tunable from 1.0 to 75 Pa. By contrast, at 60 °C a distinct gel state was obtained with an order of magnitude larger storage modulus values from 110 to 900 Pa upon increasing the CNC concentration from 0 to

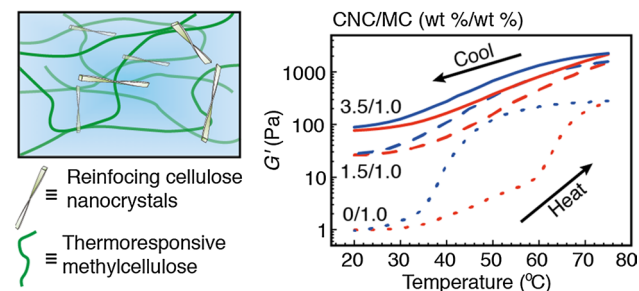


**Fig. 6** Schematic of cellulose nanocomposite hydrogel and cyclic heating of the samples with 0, 1.5, and 3.5 wt% CNC loading while keeping a fixed amount 1 wt% of methyl cellulose [50]

3.5 wt%, which is associated with the physical cross-links between MC and CNCs. This is an all-cellulose temperature responsive and tunable nanocellulose-based hydrogel.

Temperature responsive gels are greatly interest for various applications in terms of drug deliveries, tissue culture, membranes, microfluidics and sensors. By patterning and grafting PNIPAAm hydrogel films on plane substrates, arrayed valve devices have been demonstrated with up to 7800 actuated micro-cages that sequester and release solutes, along with valves actuated individually [50]. This technology is applicable for single cell handling and the nuclear acid amplification test for the Human Synaptojanin 1 gene, which is involved in several neurodegenerative diseases.

Specialized plant tissues, such as the epidermis of a leaf covered with stomata, consist of soft materials with deformability and electrochemical properties to achieve specific functions in response to various environmental stimuli. Inspired by the stimulus-responsive functionalities of plants, a new thermo-responsive multifunctional hybrid membrane was synthesized through the in situ hybridization of conductive PPy on a photopolymerized PNIPAAm matrix [51]. The hybrid membrane can be easily fabricated into various structures by smartly utilizing photopolymerization patterning and it exhibits a thermo-responsive material, which is promising platform for fabricating a variety of functional devices.

## 2.3 Photo Responsive

Photo responsive polymers commonly respond to light energy by way of a variety of degradation and bonding reactions. However, they are unanimously governed by the Planck–Einstein relation. Photo-dependent reaction rates have shown strong correlations to the energy and irradiance of light, with little variation [52]. This makes photo-catalyzed reactions an attractive mechanism for hydrogel manipulation. The major downfall with photo-induced changes comes in vivo models. Due to the inability of ultraviolet and visual electromagnetic wavelengths to penetrate tissue, these mechanisms are only really viable for ex vivo systems and skin level treatments. Recent advances with near infrared wavelength sensitive reactions have opened up some possibilities [31]. A photo responsive supramolecular actuator was designed by integrating host–guest interactions and photo switching ability in a hydrogel [53]. A photo responsive supramolecular hydrogel with a-cyclodextrin as a host molecule and an azobenzene derivative as a photo responsive guest molecule exhibits reversible macroscopic deformations in both size and shape when irradiated by ultraviolet light at 365 nm or visible light at 430 nm. Irradiating with visible light immediately restores the deformed hydrogel. A light-responsive PNIPAAm incorporating reduced graphene oxide (PNIPAAm/rGO) was achieved by the chemical

reduction of GO dispersed in the hydrogel matrix so as to avoid the problem of rGO restacking in aqueous solution [54]. Due to the enhanced photothermal efficiency of the rGO, the prepared PNIPAAm/rGO underwent large volume reductions in response to irradiation by visible light of modest intensity. With respect to potential applications, bilayer-type photo-actuators comprising a PNIPAAm/rGO active layer and PAAm passive layer were fabricated; these achieved a full bending motion upon visible-light, for example sunlight, exposure. Figure 7 shows the sunlight-driven actuator [54].

In nature, plant tendrils can produce two fundamental motion modes, bending and chiral twisting distortions, under the stimuli of sunlight, humidity, wetting or other atmospheric conditions. A dual-layer, dual composition polysiloxane-based liquid crystal soft actuator strategy was demonstrated to synthesize a plant tendril mimic material capable of performing two different three-dimensional reversible bending versus chiral twisting through modulation of the wavelength band of light stimuli (ultraviolet vs near-infrared) [55]. This material has broad application prospects in biomimetic control devices. To overcome the slow kinetics of the volume phase transition of stimuli-responsive hydrogels as platforms for soft actuators, thermally responsive

comb-type hydrogels were prepared using synthesized PNIPAAm macromonomers bearing graft chains [56].

Hygro induced motion is a fundamental process of energy conversion essential for applications that require contactless actuation in response to the day–night rhythm of atmospheric humidity. Mechanical bi-stability caused by rapid and anisotropic adsorption and desorption of water vapor by a flexible dynamic element that harnesses the chemical potential across very small humidity gradients for perpetual motion, was effectively modulated with light [57]. The element can lift objects ~85 times heavier and can transport cargos ~20 times heavier than itself. Having an azobenzene-containing conjugate as a photoactive dopant, this entirely humidity driven self-actuation can be controlled remotely with ultraviolet light.

## 2.4 Electrical Responsive

The pioneering work on electrical responsive gels was performed by Osada et al. [58] Using a PAMPS hydrogel with low crosslinking density of *N,N*-methylene bisacrylamide immersed in a surfactant solution (n-dodecyl pyridinium chloride), the gel was able to walk through a solution by alternately applying and reversing a 20 V potential at 2 s intervals. The mechanism by which this occurred was explained as “a reversible and cooperative complexing of surfactant molecules on the polymer gel in an electric field, causing the gel to shrink” and bend. Electrical responsive gels were also developed by utilizing nonionic polymer gels and dielectric liquid patterns, such as poly(vinyl alcohol)/dimethylsulfoxide (PVA/DMSO) [59, 60] and poly(vinyl chloride)/di-*n* butylphthalate (PVC/DBP) [61]. Hydrogels based on PVA/DMSO or PVC/DBP have shown the ability to exhibit electrically-induced responses of up to 8% strain, as well as bending of up to 180° within a time frame of only 90 ms. A PVA/DMSO gel achieved motility of up to 14.4 mm/s in a path-controlled manner in air by application of a 400 V/mm electric field [59]. The linear or complex responsive motion of these gels can be controlled when alternating the DC electric field, which is facilitated by the spatially varying shear forth between the dielectric liquid and gels. Angular movements of gelatin/alginate interpenetration gel membrane were achieved under non-contact DC electric field, in which the bending speed and strain can be controlled by the gel chemical composition and applied voltage [62]. These gel systems are capable of converting electromagnetic energy into mechanical energy, thus mimicking locomotion of organisms under external electromagnetic stimulus. However, limitations of the liquid electrolyte environment and low-responsive efficiency are drawbacks [43].

Soft hydrogel walkers with electrical driven motility for cargo transport have been developed via a facile mold-assisted strategy [63]. The hydrogel walkers consisting of

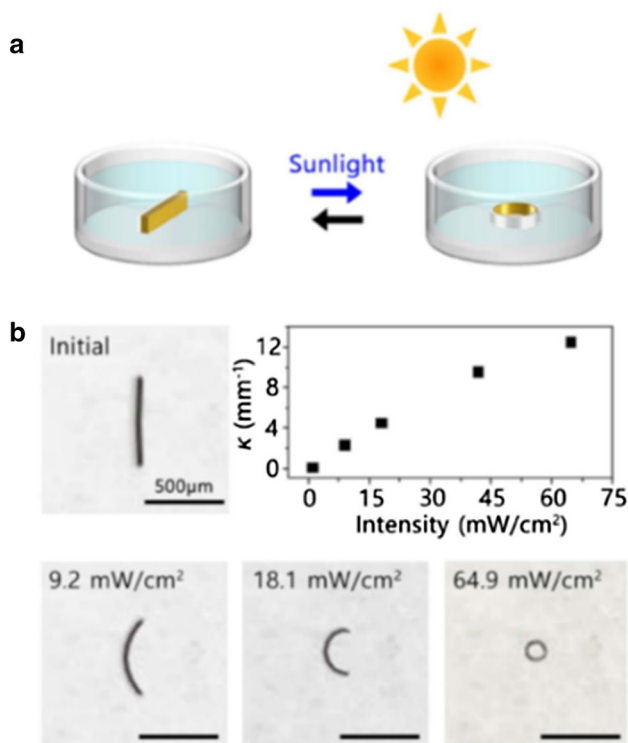


**Fig. 7** The sunlight-driven actuator: **a** schematic diagram for the sunlight-driven actuation test, **b** photographs of sunlight-driven actuation and curvature,  $\kappa$ , changes depending on the intensity [54]

polyanionic poly(2-acrylamido-2-methylpropanesulfonic acid-co-acrylamide) exhibit an arc looper-like shape with two “legs” for walking. Such hydrogel systems create new opportunities for developing electro-controlled soft systems with simple design/fabrication strategies in the soft robotic field for remote manipulation and transportation.

Ionogel electrolytes can be fabricated for electrochemical actuators with many desirable advantages, including direct low-voltage control in air, high electrochemical and thermal stability, and complete silence during actuation. A cross-linked supramolecular approach was adopted to prepare tough nanocomposite gel electrolytes from HEMA, BMIMBF<sub>4</sub>, and TiO<sub>2</sub> via self-initiated UV polymerization [64]. The tough and stable ionogels are emerging to fabricate electric double-layer capacitor-like soft actuators, which can be driven by electrically induced ion migration. The ionogel-based actuator shows a displacement response of 5.6 mm to the driving voltage of 3.5 V. The actuator can not only work in harsh temperature environments (100 °C and 210 °C) but also realize the goal of grabbing an object by adjusting the applied voltage. Figure 8 shows the schematic of the tough nanocomposite ionogels and ion transfer mechanism. [64]

Reconfigurable lens provides variable-focus in optics without any moving part. The material for a reconfigurable lens should be deformable in the presence of electrical stimuli meanwhile maintaining its optical transparency for the lens function. Poly(acrylic acid)-Poly(vinyl alcohol) (PAP) hydrogels were synthesized and characterized for reconfigurable active lens [65]. The PAP hydrogels were prepared by free radical and freeze-thaw

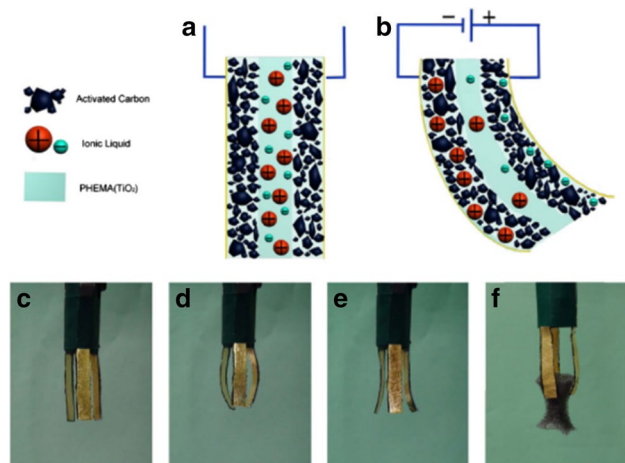


**Fig. 8** Schematic diagram of BMIMBF<sub>4</sub> gel-electrolyte-based actuator or based on an ion transfer mechanism: **a** the electric-double-layer formed inside the porous media of activated carbon, **b** strain of the actuator under an applied voltage, **c** the model of the robot manipulator, **d** under an applied voltage, **e** Under an inversely applied voltage, **f** photograph of the robot manipulator grabbing an object (180 mg) [64]

technique using *N,N*1-methylenebisacrylamaide and potassium persulfate/*N,N,N*1,*N*1-tetramethylethylenediamine as crosslinker-initiator pair system. Displacement output increased with increasing the voltage and the maximum displacement output of 15.5 μm was achieved in the presence of electrical field, which corresponds to 4% strain. PAAm was used for matrix material to fabricate composite hydrogels reinforced with natural CNC [66]. The CNC played a role as a reinforcing filler and a multifunctional cross-linker in the hydrogel. Reconfigurable lens is a niche application of electrical responsive gels.

## 2.5 Chemical Responsive

Another broad class of hydrogels is designed to exhibit swelling or degradation in response to individual target molecules [31]. Because of the wide array of chemicals which could act as practical stimuli for achieving useful functions, a few examples of chemically-responsive hydrogels are shown. The mechanisms either make use of the activity of the target molecule itself, as with using peptide-based hydrogels that degrade in response to the target enzyme or use a transduction pathway to convert recognition of the target molecule into a pH, temperature, or electrical charge change that drives swelling, collapse or degradation. Glucose-responsive hydrogels respond to the presence of elevated levels of glucose and have obvious uses in the treatment of diabetes. Hydrogels that are capable of acting as long-term insulin depots that respond to increased blood glucose levels and automatically release doses of insulin at appropriate times are a promising development, and could obviate the need for frequent injection and therefore provide a more convenient treatment option that would improve treatment efficacy and quality of life for hundreds of millions of people. Glucose-responsive hydrogels have typically relied on one of three mechanisms for detecting glucose and responding appropriately [67]. The first of these is to use glucose oxidase (GOx) as a detecting enzyme and its reaction with glucose as a transduction pathway for stimulating response. The second mechanism for glucose-responsiveness relies on the use of lectins, primarily concanavalin A (Con A). As glucose diffuses into the polymer matrix, the glucose competitively binds with Con A because Con A has greater affinity for glucose than for the glycosylated moieties. The last mechanism for glucose-responsive hydrogels is based on use of phenylboronic acid (PBA) functionalized hydrogels. PBA has ability to bind by forming reversible, covalently linked complexes with diols. When glucose, with its diol functionality, enters the hydrogel, the PBA moieties reversibly complex with glucose, shifting equilibrium toward cationically charged boron residues. The reaction shifts the overall gel charge density toward cationically charged residues. This increased charge endows the hydrogel with greater hydrophilicity, which



leads to a distinct swelling response. PBA-based hydrogels have become the most promising candidates for clinical use because they can offer sensitive glucose responsiveness.

In addition to glucose-responsive hydrogels, hydrogels can also be made to respond by being directly acted upon by the target molecule. This is most notable in the design and use of enzyme responsive hydrogels. Among the possible methods for making enzyme-responsive hydrogels, one of the well-studied methods has been to use peptide chains as linkers, either as crosslinks within the hydrogel or as links between the polymer backbone and drug molecules. These peptides are typically made of short sequences chosen to be specifically digestible to certain enzymes, causing degradation of the hydrogel in the presence of the targeted enzyme [68]. Molecularly imprinted polymers (MIPs) make use of hydrogels formed in the presence of a template molecule in order to produce binding sites that will later recognize the target molecule. MIPs are a promising method for yielding similar results as antibodies or aptamers in multiple applications [69]. MIPs therefore bear mention as an important and expanding class of chemically responsive hydrogels. The possible applications of MIPs are for use as inexpensive diagnostics or sensors, drug delivery and sorbents.

Electrochemical actuators directly converting electrical energy to mechanical energy are critically important for artificial intelligence. However, their energy transduction efficiency is always lower than 1.0% because electrode materials lack active units in microstructure, and their assembly systems can hardly express the intrinsic properties. A molecular-scale active graphdiyne-based electrochemical actuator was reported with a high electromechanical transduction efficiency of up to 6.03%, exceeding that of the best-known piezoelectric ceramic, SMA and electroactive polymer reported before, and its energy density ( $11.5 \text{ kJ m}^{-3}$ ) is comparable to that of mammalian skeletal muscle ( $\sim 8 \text{ kJ m}^{-3}$ ) [70]. The actuator remains responsive at frequencies from 0.1 to 30 Hz with excellent cycling stability over 100 k cycles. The alkene–alkyne complex transition effect is responsible for the high performance through in situ sum frequency generation spectroscopy. Figure 9 shows the actuation of the graphdiyne-based electrochemical actuator.

### 3 IPMCs

Generally, EAPs are divided into two major categories based on their activation mechanism: electronic (driven by electric field or Coulomb forces) and ionic (involving mobility or diffusion of ions). The electronic polymers, such as electrostrictive, electrostatic including dielectric, piezoelectric, and ferroelectric require high activation field close to the breakdown level [3]. In contrast, ionic EAP materials, such as gels, polymer-metal composites, conductive polymers,

and carbon nanotubes require low actuation voltage. However, there is a need to maintain their wetness, and except for conductive polymers it is difficult to sustain dc-induced displacements. Ionic polymer metal composites (IPMCs) are an important type of ionic EAPs [71]. IPMC is composed of a core ion-conductive polymer membrane including mobile molten ionic salts and noble metallic electrodes. The bending motion of IPMC occurs via the redistribution of mobile ions toward the oppositely charged electrode surface under electric field. Since Oguro et al. [72] firstly have found the bending phenomenon for the Nafion<sup>®</sup> plated with platinum activated by a small voltage in 1991, many attempts were made on depositing metal electrodes and choosing ionic polymers including counter cation species, which resulted in performance improvement. The alkyl ammonium ion incorporated ionic polymers have larger deformation and a lower rate than the alkali metal ion incorporated polymers [73–75]. As for the corresponding actuation mechanism of IPMC, the ion transport properties and electro-mechanical properties of ionic polymers play key roles in defining actuator performance [76]. Therefore, high-performance IPMC actuators should be functionally designed and fabricated to have a micro-/nano-morphology network in a polymer matrix with hydrophilic nano-channels, microphase-separated morphology, and/or well-dispersed pore structure, highly conductive molten ionic salts, and flexible electrode materials. Typical ionic polymer actuators suffer from significant drawbacks such as stress relaxation under a step input, low blocking force and durability, environmental unfriendliness and high cost of fabrication due to the usage of fluorinated polymers and noble metallic electrodes through a very complex and time-consuming electro-less plating process. To overcome these problems, many ionic polymers have been proposed including sulfonated hydrocarbon polymers, self-assembled sulfonated polyimide block copolymers, functionalized cellulose-based biopolymers and smart carbon-based nanocomposite membranes [77–82]. Many actuators and robots have been developed with IPMCs as actuators and sensors including flexible brail display, soft bio-inspired fin, biomimetic Venus flytrap and flow measurement sensor [83–89]. Recently an ionic polymer-metal composite actuator having multiple-shape memory effect was reported, which is able to perform complex motion by two external inputs, electrical and thermal [5]. Figure 10 shows the multiple-SMP metal composite (MSMPMC) actuator that shows bending and twisting at the same time by electric field and temperature.

### 4 Conducting Polymers

CPs typically function via the reversible counter-ion insertion and expulsion that occurs during redox cycling. CPs are semiconductor or insulator as the conductivity

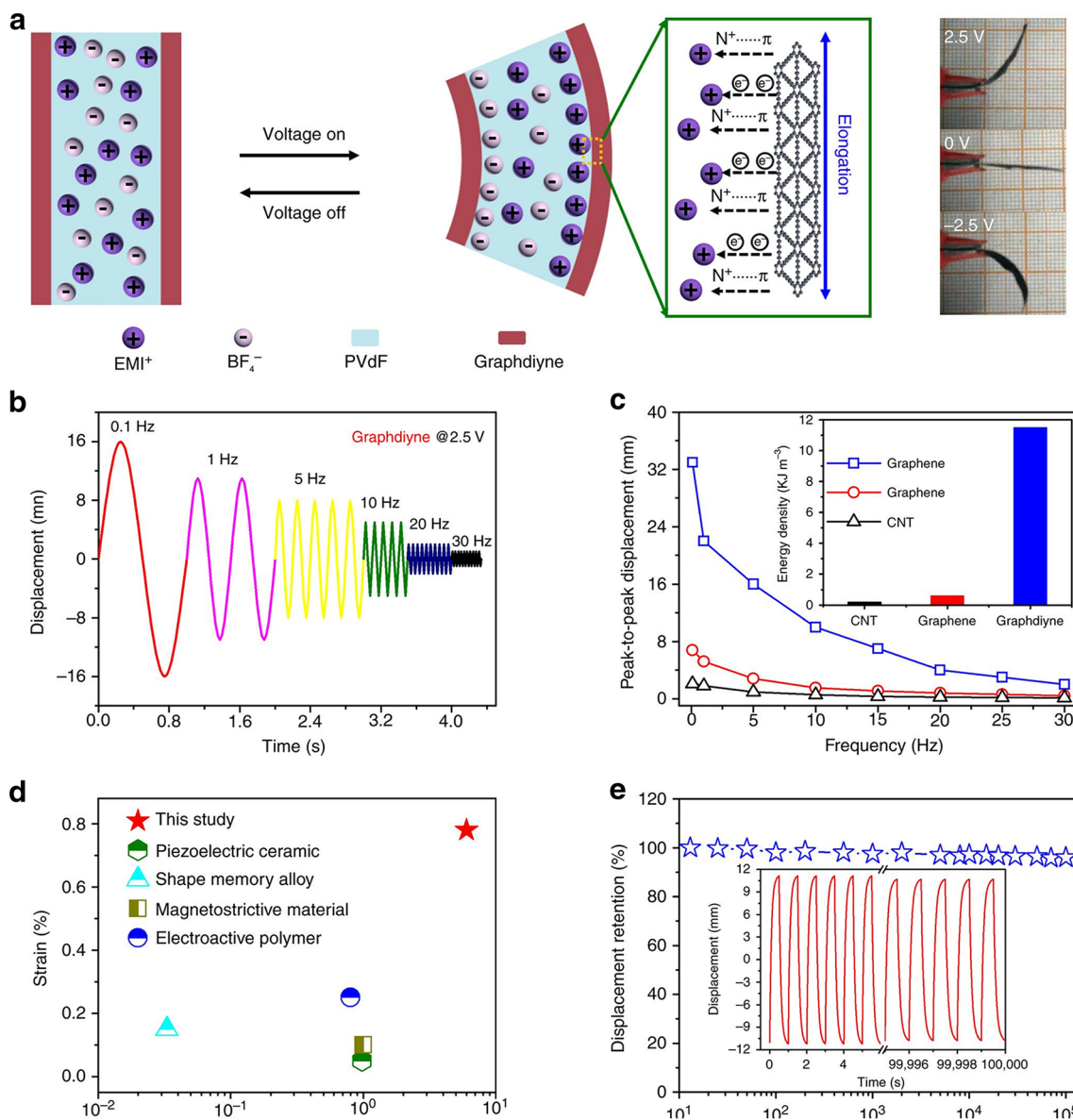


**Fig. 9** Actuation performance of the graphdiyne actuator: **a** schematic for actuation mechanism of the actuator. Optical images show the bent actuator under 2.5 V at 0.1 Hz. **b** Actuation strain of the actuator with increasing frequency. **c** Peak-to-peak displacement as

a function of frequency. Inset is the comparison of their power densities. **d** Comparison of transduction efficiency of different types of actuation materials. **e** Cyclic stability of the actuator. Inset shows the actuation cycles [70]

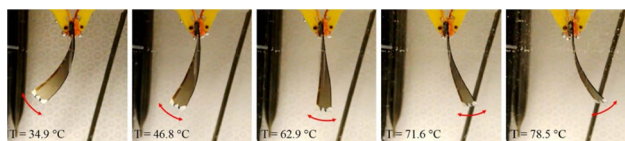


**Fig. 10** A MSMPMC actuator with multiple dof deformation. The sample was under a sinusoid AC voltage of 3.7 V and 1 Hz [5]

increases markedly upon oxidation [90]. The oxidation is carried out by exposure of CPs to oxidizing agents or by electrochemical oxidation. During oxidation CPs are

swollen by insertion of bulky ion. CPs are soft and flexible, mechanically tough and high conductivity, which are suitable to electrically controllable soft actuator. CP actuators are available as films, filaments/yarns and textiles, operating in liquids as well as in air. Most studies on CPs have been done on PPy, polyaniline, polythiophene and poly(3,4-ethylenedioxythiophene). Since they are aromatic structure in the unit molecule, hence, generally they are stable polymers compared with linear polymer. The PPy is the most studied CP for actuators because it is easily electrodeposited on appropriate metal electrode and is

obtained as high conductive and tough films. PPy can be prepared as compact film or porous gel-like film. Furthermore, the PPy film exhibits a large electrochemical strain of 39% [91] and a force of 49 MPa [92] at the optimized condition in actuation, and a long cycle life [93].

Great progress has been made in understanding these materials and the actuation mechanisms [90, 94]. CPs are obtained by either chemical or electrochemical oxidative polymerization of monomers. The oxidized state is swollen by the total volume of inserted anions and stiffened due to the ionic crosslink. The ionic crosslink is formed by the ionic bonding between polarons and anions, resulting in fastening inter-polymer chain bonding. When a small anion is employed, the anion can be ejected during reduction and the CP shrinks [95]. Upon oxidation, the CP expands. In this case, the in-migration ions are anions. On the other hand, if a large anion is employed in the synthesis, the large anion is immobilized inside of the polymer, and the CP is reduced by inserting cations to neutralize anions. The reversible expansion of PPy films that occurs on redox switching is primarily the result of ion movements [96] and that different ion transport modes can operate depending on the size of the dopant ion [97]. Note that the oxidized state is mechanically stiffer than that of the reduced state by about 2–3 times [98].

The reversible volume change of CP can be used as the active part in a soft actuator with various configurations that lead to different motions such as bulk, linear, bending bilayer, buckling and bending trilayer as shown in Fig. 11. The volume change is typically isotropic and can be used as a bulk actuator. Linear deformation can be easily achieved by designing CPs as free-standing films, strips, or fibres. Intrinsically linear actuators working in air have been made. Actuators based on a CP fibre or film, embedded in a SPE and using a metallic electrode as counter electrode were proposed by several groups [41, 42]. With this idea, a linear actuator can be fabricated by laminating CP layers on an inert stretchable film. The volume change of CPs can also be used to achieve out-of-plane movement by designing the actuator in a bilayer configuration to produce bending actuators. Bilayer actuators are made by laminating CP layer and passive thin film, in which the relative expansion or contraction of the CPs with respect to the other passive

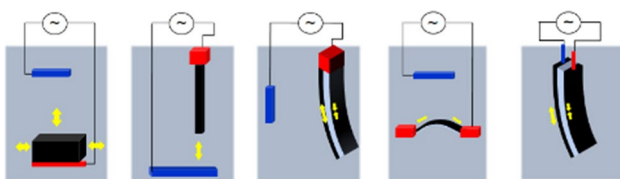


**Fig. 11** Various configurations of CP soft actuators: bulk, linear, bending bilayer, buckling and bending trilayer in electrolyte

layer leads to a bending of the structure. Trilayer actuators are comprised of a passive layer sandwiched by two CP layers and are relatively easy to fabricate [52].

The inherent volume change properties of CPs result in interesting opportunities for applications. They can not only be actuated in biological electrolytes, but actively use the surrounding media as the ion source resulting in a simpler device geometry. This allows their use in medical devices and in applications in cell biology, organic bioelectronics, active catheters for the vascular system and cochlear electrode array [99–102]. A microrobotic arm and manipulator, microfluidics, smart pill, microvalve [31], tactile transducer [103] were demonstrated with CPs [104–107]. Bending trilayer microactuators can also be used to drive flapping wings for artificial insects, or micro-unmanned aerial vehicles [108].

CPs are known to be attractive for their low operating voltage, large strain, large contraction force, possibility of microfabrication and easy preparation in the optimized circumstance, in comparison with other EAPs. However, there are still limitations prior to commercialize CP actuators, such as slow response, need for an electrolyte source, encapsulation and low electromechanical coupling efficiency. Creeping is a phenomenon that is observed as the irreversible and uncontrollable elongation, when the tensile load stress goes over the elastic region. In soft actuators the creeping is a serious problem for the precise positioning [93]. The creeping in CPs is caused by uniaxial alignment of polymer chains, slipping of polymer chains and partial breaking of polymer chains before the breakdown of CP actuators. Evaporation of the aqueous or organic electrolyte solutions degrades the performance of CP actuators. Thus, encapsulation for the actuators is necessary. However, encapsulation by using polymers has not been fully successful. Surprisingly, IL provide a much better solution as the electrolyte in CP actuators, which enhance the lifetime and stability of CPs without encapsulation [109]. Another issue restricting the lifetime of CP actuators is the delamination between the active CP layer and passive layer due to the relatively poor adhesion between them.

## 5 CNTs and Graphene

Materials based on carbon are various: graphite, diamond, carbon fibers, fullerene, carbon nanotubes and graphene. All this is possible because carbon forms various types of bond. It has been also known that charging/discharging of single-wall carbon nanotubes (SWNT) results in substantial changes in the lengths of the individual nanotubes [110]. These dimensional changes are useful for converting electrical energy to mechanical energy in soft actuators. The SWNT soft actuators show very promising actuation

properties in relation to their high surface area, excellent mechanical properties and the non-faradic nature of the electrochemical response leading to long life. They are able to produce high strain and stress in the presence of low actuation electric field. Their actuation mechanism is based on quantum-chemical effects induced by the double layer charge which is produced at the interface between nanotube and solution [110]. Changing the applied potential, an electronic charge is stored in the SWNT, and it is compensated by the ions at the interface carbon nanotube/solution, creating the double layer. This charge accumulation causes the quantum chemical and electrostatic effects, which in turn determine the dimensional and stress changes. Changing the applied voltage results in double-layer charge injection for very high surface-area electrodes. Quantum chemical effects cause the carbon–carbon bond lengths to change as the amount of injected charge is varied, which provides the changes in nanotube dimensions. Large actuator effects arise because large amounts of charge can be stored in the electrochemical double layer that results when the nanotubes are immersed in an electrolyte and an electrochemical potential applied. Aligned Multiwall-carbon nanotube (MWNT) arrays exhibited an electromechanical actuator response [111]. The actuator mechanism is quite different from the quantum chemical mechanism of bond elongation occurring for SWNT mats in which the tube axis is preferentially in the sheet plane. The new mechanism appears to be expansion on charging due to the repulsion of electrical double layers associated with individual multi-wall carbon nanotubes.

A potential advantage of CNT actuators, in comparison to other solid state actuators, is the extremely high stress generation that should eventually be achievable with nanotubes. For the achievable actuator strain of 1%, the individual nanotubes should generate a stress of 6 GPa, which is several orders of magnitude higher than for other actuators [112]. Giant work capacities and high strain rates are also predicted for actuators that can utilize the mechanical properties of the individual nanotubes. However, realization of these performance advantages requires the major improvements in the utilization of nanotube mechanical properties in nanotube assemblies. Furthermore, their response is slow and there is a need to maintain their wetness, and except for conductive polymers it is difficult to sustain dc-induced displacements.

Spinning of MWNTs has been investigated [113] and recently it has been shown that highly twisted MWNT yarns produce a unique mechanical actuation involving coupled rotation and axial contraction [114, 115]. The torsional and tensile actuation is achieved by reversible yarn volume changes driven by electrolyte ion influx/release during electrochemical charge/discharge, or thermal expansion/contraction of a guest material, like paraffin wax. These soft actuators can generate rotation per length over 1000 times

higher than previously reported torsional actuators made from shape-memory alloy, piezoelectric ceramics and CPs. However, there are important challenges in electrochemically driving MWNT yarns actuators. If liquid electrolyte is used, the weight and volume of electrolyte and liquid containment system can be much higher than for the actuating yarn, leading to low volumetric and gravimetric performance for the actuating system. All-solid-state MWNT yarns were developed, which are electrochemically driven so as to avoid the above problems [116].

Electrolyte-infiltrated and twisted, coiled MWNT anode and cathode yarn muscles yarns were plied together to jointly provide torsional and tensile actuation when operated in ambient air. The maximum realized tensile stroke (1.3%) is a little higher than previously reported for an electrochemically powered, twisted carbon nanotube yarn muscle that actuates in a liquid electrolyte bath [115]. Figure 12 shows the yarned MWNT for torsion and tensile actuation [116].

## 6 Dielectric Elastomers

As soft and flexible electrical insulators, DEs can express mechanical motions in response to electrical stimulation: when a dielectric membrane is subjected to a voltage across its thickness, the membrane suffers an electrostatic force, the so-called Maxwell stress, and thus squeezes in the thickness direction and expands in the area direction [117]. DE based EAPs have been developed during last three decades. DEs are rubbery polymer materials with compliant

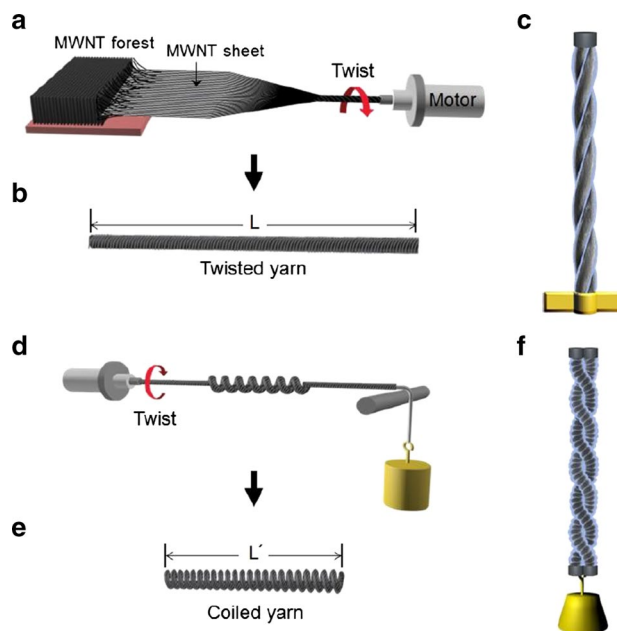


Fig. 12 Illustration of yarn fabrication for torsion and tensile actuation [116]

electrodes that have a large electromechanical response to an applied electric field. The induced strain is proportional to the square of electric field, multiplied by the dielectric constant and inversely proportional to the elastic modulus. Use of polymers with high dielectric constants and application of high electric fields lead to large forces and strains. The deformation of the polymer film can be used in many ways to produce actuation. A linear artificial muscle was made based on an acrylic-film double bow-tie actuator. An acrylic film rolled actuator was developed and applied to an insect-inspired legged robot. An insect-inspired flapping-wing robot was demonstrated by using four silicon bow-tie actuators. DEs can also be used for sensors and energy harvesters [118, 119]. A new type of contractile polymer-based electromechanical linear actuator was developed by utilizing DEs [120]. It is based on a novel helical configuration, suitable for the generation of electrically driven axial contractions and radial expansions. An axial strain of  $-5\%$  at about  $14 \text{ V}/\mu\text{m}$  was obtained from first prototypes.

The critical problem of DEs is that they need high voltage for activation, which results in high electrical strain related difficulties, such as voltage breakdown shielding, packaging, miniaturization, and driver configuration in device implementations. Improving the dielectric constant and lowering the elastic modulus of the polymer dielectrics are possible ways of lowering the actuation voltage. All-polymer percolative composite was developed which exhibits a very high dielectric constant [121]. Since the actuation force output is increased with the stiffness of DEs, the stiffness should be optimized. An important factor governing the performance of DE actuators is the nature of the electrodes [122]. The electrodes need to exhibit sufficient electrical conductivity and low elastic modulus that does not block the actuation. Compliant electrodes made of carbon grease or graphite powder have been commonly used because they combine electrical conductivity with negligible elastic modulus. Despite enabling high actuation amplitudes, these electrodes exhibit poor structural stability. All-polymeric actuators with “solid” composite elastomer electrodes have been studied to overcome such limitations without sacrificing actuation performance [122].

DEs with optical transmittance are emerging materials with practical significance in next-generation flexible displays, flexible touchscreen panels and smart optics. Flexible and transparent DE with high dielectric constant and transmittance over 90% have been reported [74, 123–125]. Figure 13 shows dielectric constant plotted against elastic modulus and transmittance with respect to dielectric constant of DEs (replotted and revised from Reference 73). CPPU is cellulose nanocrystal based transparent and electroactive polyurethane [125].

Soft actuators can be made by applying electric field on the dielectrics. Dielectric gels are attractive because

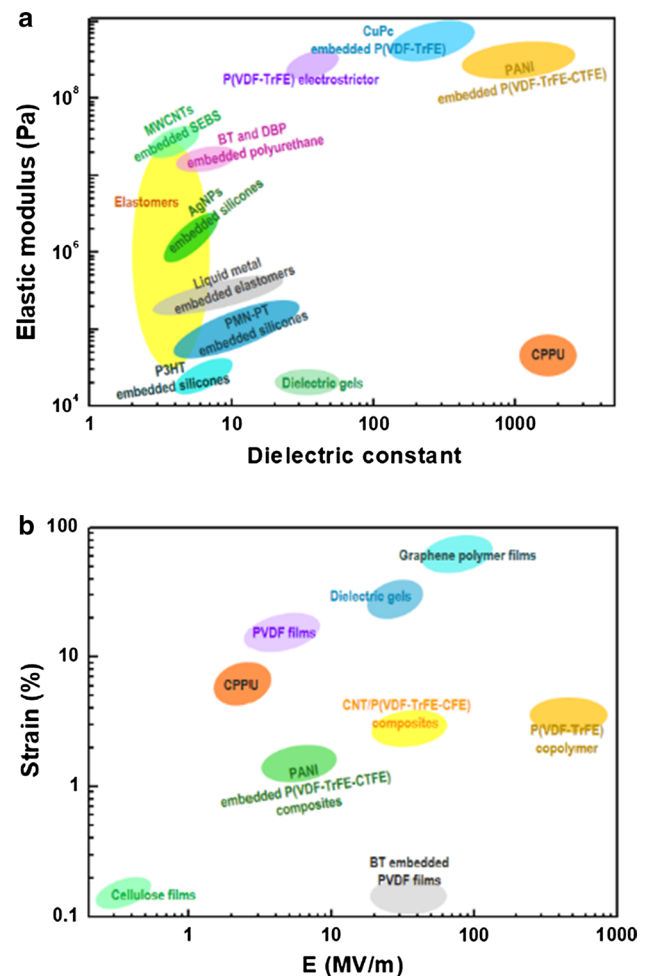


**Fig. 13** **a** Elastic modulus of DEs with respect to dielectric constant and **b** transmittance versus dielectric constant of DEs (replotted and revised from Reference [73])

of their softness. The force output directly proportional to dielectric constant of the gels. Thus, high dielectric constant is essential for high performance dielectric gels. A new type of polymer-based dielectric gel was reported, which has ultra-high dielectric constant ( $\epsilon = 30\text{--}50$ ), low elastic modulus ( $20\text{--}60 \text{ kPa}$ ) and excellent transparency ( $\sim 99\%$ ) [126]. The dielectric gel was designed by using solvents with ultra-high  $\epsilon$  and a polymer network that matched well with the solvents, which exhibited high stretchability ( $\sim 10$  times) and low mechanical hysteresis. By using the dielectric gels, a bioinspired tunable lens was demonstrated of which the focal length of which can be adjusted by varying the applied voltage. The dielectric gels offer new opportunities for soft robotics, sensors, electronics, optics, and biomimetics. However, dielectric constant measurement for dielectric gels is controversial. A broadband dielectric/impedance spectrometer (Novocontrol GmbH) the testing copper electrodes was used to measure the dielectric constant of gels.

The gel samples were treated without metal sputtering on their surfaces. In this measurement configuration, the measured dielectric constant may exhibit a variation depending on the solvent or water content of the gels and the interface impedance between the electrodes and gels. Thus, instead of directly measuring dielectric constant of gels, an electromechanical performance of gels was measured and dielectric constant can be conversely calculated [127–129]. The strain induced by the Maxwell stress along the applied-field direction is given by [121]

$$s = \frac{1}{2} \epsilon_0 \epsilon_r E^2 \frac{1 + 2\mu}{Y} \quad (1)$$

where  $\epsilon_0$  is free space permittivity ( $8.85 \times 10^{-12}$  F/m),  $\epsilon_r$  is the relative dielectric constant of gel and  $E$  is electric field strength,  $\mu$  is Poisson's ratio and  $Y$  is Young's modulus. By using Eq. 1, the relative dielectric constant of gels can be estimated as shown in Table 2. As one can see, the estimated dielectric constants from the electromechanical strains for PAAm-PVC, PAAm/CNC, PVA/Cell and PVA/PAAm hydrogels are larger than the reported ACOMO-MBA gel. This might be attributed to a motion of free charge carriers due to charges present on the CNC surface and interfacial polarization effects. However, their actuation principle might not be solely associated with electrostatic effect. Further discussion on the actuation principle of soft actuators will be made in later section.

## 7 Shape Memory Polymers

SMPs are a kind of smart materials, which can be deformed into temporary shapes and restore their permanent shapes by external stimuli on demand such as heat, light, electric field, magnetic field or moisture [130, 131]. SMPs typically consist of two elements: switching units and netpoints [132]. The switching units are responsible for controlling shape fixity and recovery, and the netpoints determine the permanent shape of SMPs. Netpoints can be chemical in nature, as in covalently connected polymer segments in cross-linked networks. They can also exist as physical cross-links, as has been realized in block-copolymer-based SMPs.

Two-way SMP (2W-SMP) represents a special class of SMPs [130]. Features make 2W-SMP so unique and attractive include: (1) 2W-SMP behaves thermally opposite to common physics, i.e. expands upon cooling (EUC) and contracts upon heating (CUH); (2) the expansion and contraction in response to temperature change can undergo reversible cycles in a continuous mode once triggered. Since two-way shape memory effect (2 W-SME) was initially reported in 2001 for liquid crystalline elastomers, this effect has been reported for a semicrystalline polymer network-crosslinked poly(cyclooctene), poly( $\epsilon$ -caprolactone)6–13, oligo(pentadecalac-tone), ionomer Nafion, poly(octylene adipate), poly(ethylene-co-vinyl acetate), polyurethane, and more. Owing to the intriguing properties of 2W-SMPs, soft actuators, morphing structures, fastening devices, optical gratings, grippers, fixators, swimmers, and artificial muscles can be designed. However, the previously developed 2W-SMPs have limitations in terms of working temperature and low tensile strength and stiffness. One of the ways to overcome this drawback is to prepare composites by introducing inorganic nanofillers into polymers. A thermo-responsive and water-responsive SMP nanocomposite network was made by chemically cross-linking CNCs with polycaprolactone and PEG [133]. The PEG–PCL–CNC nanocomposite exhibited excellent thermo-induced and water-induced SME in water at 37 °C, and the introduction of CNC clearly improved the mechanical properties of the composites, which is potentially useful for smart biomaterials. A new 2W-SMP was made with crosslinked cis poly(1,4-butadiene) that can be actuated below 0 °C with giant actuation strain [134]. A novel biodegradable polymer-based 2W-SMP was made by using poly(propylene carbonate) and microfibrillated cellulose [132].

Recent discovery of triple-shape, multiple-shape, and reversible shape memory beyond the classical dual-shape behavior has reshaped the landscape in SMP field, yet all shape memory behaviors share a common root in polymer elasticity. An opposite behavior—polymer plasticity, has recently gained attention [135]. This is achieved by covalent bond exchange in a polymer network, allowing its topography to be rearranged in response to an external force, which gives a permanent and nonrecoverable shape

**Table 2** Hydrogels and their Young's modulus, strain and dielectric constant

| Gel composition | Young's modulus (kPa) | Electric field (kV/mm) | Strain (%) | Estimated dielectric constant ( $\epsilon_r$ ) | Ref. |
|-----------------|-----------------------|------------------------|------------|--|------|
| ACMO-MBA        | 20                    | 8                      | 1.72       | 67.5 (30–50)                                   | [71] |
| PAAm-PVC        | 67                    | 0.4                    | 0.0039     | 205.0  | [63] |
| PAAm/CNC        | 56                    | 0.2                    | 0.0018     | 307.6  | [64] |
| PVA/Cell        | 170                   | 0.25                   | 0.0015     | 512.0  | [72] |
| PVA/PAAm        | 83                    | 0.4                    | 0.004      | 260.5  | [73] |
| PVA/CNC         | 7                     | 0.4                    | 0.0036     | 19.8   | [74] |

change. Permanently reshaping polymers via plasticity can be repeatedly done without losing the previous strain history, opposite to the elasticity-based SME. Among various shape-changing materials, the elastic nature of SMPs allows fixation of temporary shapes that can recover on demand, whereas polymers with exchangeable bonds can undergo permanent shape change via plasticity. The elasticity and plasticity were integrated into a single polymer network [136]. By exploring the cumulative nature of the plasticity, easy manipulation of highly complex shapes were demonstrated that is extremely challenging. Figure 14a shows that a square film can be folded plastically into a permanent bird, which can be deformed into various temporary shapes that can recover by virtue of its elasticity. Figure 14b shows that with cutting, folding, and plastic deformation, a rectangular flat film can be used to create a kirigami structure that can also be deformed into recoverable temporary shapes. The dynamic shape-changing behavior paves a new way for fabricating geometrically complex multifunctional devices.

Shape memory gels can be deformed and further altered to the original shape when exposed to external stimuli. Temperature-driven memory shape gels are typically prepared by copolymerization of acrylic acid with n-stearyl acrylate [137], which are able to render the original shape below 50 °C. This is facilitated by long alkyl chains of stearyl acrylate that adopt crystalline aggregates to maintain mechanical properties. Above 50 °C, the gel becomes soft and flexible as the side chain conformations are disordered. The order–disorder transitions which are associated with the formation of crystalline aggregates along the side chains are responsible for deforming and recovering of the original shape. Another class of shape memory gels is based on the partially interpenetrating PNIPAAm gels with PAAm

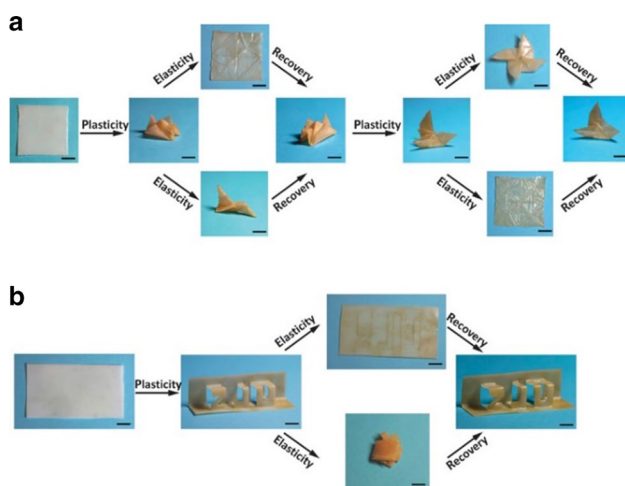


**Fig. 14** Shape manipulation via thermally distinct elasticity and plasticity: **a** smart origami structures. **b** Smart kirigami structure. Scale bars 10 mm [136]

[138]. The resultant gels possess internally heterogeneous and modulated structures, which are responsible for spatial shape modulation. The controlling mechanism is the temperature sensitivity of PNIPAAm and solvent (acetone) concentration sensitivity of PAAm. At elevated temperatures or higher acetone concentrations, the bigel strip bends to a circle. This concept can be further applied to PAAm bigels modulated by pH changes [43].

## 8 Biopolymers

The use of renewable materials is essential in future technologies to harmonize with our living environment. Renewable materials can maintain our resources from the environment so as to overcome degradation of natural environmental services and diminished productivity [139, 140]. Biopolymers, obtained from nature, belongs to renewable materials. The use of biopolymers is essential for achieving sustainability in future technology. There are many biopolymers, for example, cellulose, chitin, bamboo, cork, hemp, coconut palm, algae, and so on [141]. Their recent advancement for smart material applications has been reviewed [139, 142]. The excellent and smart characteristics of cellulose materials, such as lightweight, biocompatibility, biodegradability, high mechanical strength/stiffness and low thermal expansibility, have made cellulose a high potential material for various industry applications. Cellulose has recently been discovered as a smart material in the electroactive polymers family which carries the name of cellulose-based electroactive paper (EAPap) [143]. The actuation phenomenon is known to be the combination of piezoelectricity and ionic transport in the cellulose. Two distinctive natures of EAPap can be made: piezoelectric and ionic EAPap. The piezoelectric EAPap, termed as Piezopaper, can produce deformation at high frequency up to audible ranges but its deformation is small since it is caused by the ordered domain of cellulose including crystalline of cellulose. On the other hand, ionic EAPap can produce a large deformation at relatively low frequency ranges since it is produced by an ion migration associated with mobile and fixed ions in cellulose materials. Intentionally ions can be added the cellulose material, for example by absorbing ionic liquid in it, so as to extensively enhance its ion migration effect without encapsulation in room humidity and temperature [144]. This kind of ionic EAPap can be used for remotely driven biomimetic actuators [145]. Cellulose possesses very systematic structure. Cellulose chains are systematically packed in such a way that they form crystal parts, so called CNC, meanwhile amorphous and crystal parts of cellulose are sequentially located along the fiber direction in a row, which is so called cellulose nanofiber (CNF) [40]. It is almost impossible to break the crystal parts of cellulose because of strong hydrogen

bonding between hydroxyl groups in CNC. CNC and CNF are called nanocellulose (NC). As well as being completely renewable, safer to handle, and cheaper to produce, NC also possesses exceptional physical and chemical properties including high elastic modulus, dimensional stability, low thermal expansion coefficient, outstanding reinforcing potential and transparency. Applications of NC are getting broad [146]: conventional ones include composites for automotive components, food packaging, barrier materials, transparent films, coatings, filtration membranes, pigment, additives, tissue engineering, wound dressing, drug deliver, cosmetics, and so on. High end ones are flexible electronics, electronics packaging, conductive films for sensors, actuators, translucent diffusers for optoelectronic devices, flexible solar cells, OLEDs, piezoelectric sensor, biosensors, electrolyte membranes for Li-ion batteries, paper batteries and supercapacitors [147–149]. NC is so versatile that it is considered as a ‘post-carbon’ material.

## 9 Summary

This paper reviewed all about soft actuator materials including gels/hydrogels, IPMCs, conducting polymers, carbon nanotubes/graphene, dielectric elastomers, shape memory polymers and biopolymers. Preparation, synthesis, performance and limitations of these materials are illustrated. The border line of softness for these materials was distinguished with elastic modulus in the range of GPa by the comparison with conventional actuators and other solid state actuator materials. Stimuli response gels/hydrogels can produce large deformation with various external stimuli- pH, temperature, light, chemical, electric and magnetic fields. Softness is an advantage of these materials. However, keeping wetness, low speed and hysteresis are challenges that should be overcome. Dielectric gels are shown to be promising since it has high dielectric constant, a large electrostatic force can be produced in the presence of electric field. IPMCs and conducting polymers, which are ionic actuator materials, have been successfully improved their performance by incorporating ionic liquids. Yarned CNTs can produce large strain by electrochemically, which is promising for contractile actuators. Dielectric elastomers are robust to produced large strain under high electric field. The challenges in dielectric elastomers are to develop high dielectric constant materials to reduce the actuation voltage and stretchable and flexible electrodes. Multiple-shape and reversible shape memory polymers were developed, which are attractive for tunable kirigami structures. Biopolymers are attractive for soft actuator materials since they are environment-friendly, renewable and biocompatible. Nanocellulose, a new building block of future materials, is so versatile that it can bring a new era of ‘post-carbon’.

This paper does not deal with actuation mechanisms and design ideas that utilize soft actuator materials. By better understanding advantages and limitations of these materials in conjunction with noble design ideas, soft actuator materials can be broadly applied for various applications including soft mechatronics, soft robots, medical devices, haptic devices, flexible devices and smart optics.

**Acknowledgements** This work was supported by Creative Research Initiatives Program through the National Research Foundation of Korea (NRF) funded by the Ministry of Science, Technology and ICT (NRF-2015R1A3A2066301).

## References

1. Spillman, W. B., Jr., Sirkis, J. S., & Gardiner, P. T. (1996). Smart materials and structures: what are they? *Smart Materials and Structures*, 5(3), 247–254.
2. Hollerbach, J. M., Hunter, I. W., & Ballantyne, J. (1992). A comparative analysis of actuator technologies for robotics. In O. Khatib, J. J. Craig, & T. Lozano-Perez (Eds.), *Robotics review 2* (pp. 299–342). Cambridge: The MIT Press.
3. Bar-Cohen, Y. (2004). *Electroactive polymer (EAP) actuators as artificial muscles—Reality, potential and challenges*. Bellingham: SPIE Press.
4. Carpi, F., Bauer, S., & De Rossi, D. (2010). Stretching dielectric elastomer performance. *Science*, 330(6012), 1759–1761.
5. Shen, Q., Trabia, S., Stalbaum, T., Palmre, V., Kim, K., & Oh, I.-K. (2016). A multiple-shape memory polymermetal composite actuator capable of programmable control, creating complex 3D motion of bending, twisting, and oscillation. *Scientific Reports*, 6, 24462–24472.
6. Zhang, M., Atkinson, K. R., & Baughman, R. H. (2004). Multifunctional carbon nanotube yarns by downsizing an ancient technology. *Science*, 306(5700), 1358–1361.
7. Santa, A. D., De Rossi, D., & Mazzoldi, A. (1997). Characterization and modelling of a conducting polymer muscle-like linear actuator. *Smart Materials Structures*, 6(1), 23–34.
8. Trivedi, D., Rahn, C. D., Kier, W. M., & Walker, I. D. (2008). Soft robotics: Biological inspiration, state of the art, and future research. *Applied Bionics and Biomechanics*, 5(3), 99–117.
9. Case, J. C., White, E. L., & Kramer, R. K. (2015). Soft material characterization for robotic applications. *Soft Robotics*, 2(2), 80–87.
10. Shepherd, R. F., Llievski, F., Choi, W., Morin, S. A., Stokes, A. A., Mazzeo, A. D., et al. (2011). Multigait soft robot. *Proceedings of the National Academy of Sciences of the United States of America*, 108(51), 20400–20403.
11. Tolley, M. T., Shepherd, R. F., Mosadegh, B., Galloway, K. C., Wehner, M., Karpelson, M., et al. (2014). A resilient, untethered soft robot. *Soft Robotics*, 1(3), 213–223.
12. Boyraz, P., Runge, G., & Raatz, A. (2018). An overview of novel actuators for soft robotics. *Actuators*, 7(3), 48–68.
13. Rus, D., & Tolley, M. T. (2015). Design, fabrication and control of soft robots. *Nature*, 521(7553), 467–475.
14. Elango, N., & Faudzi, A. A. M. (2015). A review article: investigations on soft materials for soft robot manipulations. *International Journal of Advanced Manufacturing Technology*, 80(5–8), 1027–1037.
15. Miriyev, A., Stack, K., & Lipson, H. (2017). Soft material for soft actuators. *Nature Communications*, 8, 596.



16. Chu, W. S., Lee, K.-T., Song, S.-H., Han, M.-W., Lee, J.-Y., Kim, H.-S., et al. (2012). Review of biomimetic underwater robots using smart actuators. *International Journal of Precision Engineering and Manufacturing*, 13(7), 1281–1292.
17. Baek, S.-M., Lee, J.-E., Yim, S., Chae, S., Jung, G.-P., & Cho, K.-J. (2018). Review of the insect-inspired robots: From single to multi-modal locomotion. *Journal of the Korean Society for Precision Engineering*, 35(10), 911–923.
18. Kim, M.-S., Song, S.-H., Han, M.-W., Chu, W.-S., & Ahn, S.-H. (2017). Fabrication of miniature high-speed actuator capable of biomimetic flapping motions. *Journal of the Korean Society for Precision Engineering*, 34(9), 597–602.
19. Koh, J.-S., Lee, D.-Y., Kim, J.-S., Kim, S.-W., & Cho, K.-J. (2013). Design and fabrication of soft deformable wheel robot using composite materials and shape memory alloy coil spring actuators. *Journal of the Korean Society for Precision Engineering*, 30(1), 47–52.
20. Cao, J., Liang, W., Zhu, J., & Ren, Q. (2018). Control of a muscle-like soft actuator via a bioinspired approach. *Bioinspiration & Biomimetics*, 13(6), 066005.
21. Shin, D.-G., Kim, T.-H., & Kim, D.-E. (2017). Review of 4D printing materials and their properties. *International Journal of Precision Engineering and Manufacturing-Green Technology*, 4(3), 349–357.
22. Pham, A.-D., & Ahn, H.-J. (2018). High precision reducers for industrial robots driving 4th industrial revolution: State of arts, analysis, design, performance evaluation and perspective. *International Journal of Precision Engineering and Manufacturing-Green Technology*, 5(4), 519–533.
23. Lee, J., Kim, H.-C., Choi, J. W., & Lee, I. H. (2017). A review on 3D printed smart devices for 4D printing. *International Journal of Precision Engineering and Manufacturing-Green Technology*, 4(3), 373–383.
24. Khare, V., Sonkaria, S., Lee, G.-Y., Ahn, S.-H., & Chu, W.-S. (2018). From 3D to 4D printing—Design, material and fabrication for multi-functional multi-materials. *International Journal of Precision Engineering and Manufacturing-Green Technology*, 5(4), 519–533.
25. Kwon, J. W., Park, H. W., Park, Y.-B., & Kim, N. (2017). Potentials of additive manufacturing with smart materials for chemical biomarkers in wearable applications. *International Journal of Precision Engineering and Manufacturing-Green Technology*, 4(3), 335–347.
26. Lee, J. S., Seol, Y.-J., Sung, M., Moon, W., Kim, S. W., Oh, J. H., et al. (2018). Development and analysis of three-dimensional (3D) printed biomimetic ceramic. *International Journal of Precision Engineering and Manufacturing*, 19(9), 1377–1384.
27. Kim, M. S., Song, S. H., Kim, H.-I., & Ahn, S.-H. (2016). Hybrid 3D printing and casting manufacturing process for fabrication of smart soft composite actuators. *Journal of the Korean Society for Precision Engineering*, 33(1), 77–83.
28. Wallin, T. J., Pikul, J., & Shepherd, R. F. (2018). 3D printing of soft robotic systems. *Nature Reviews Materials*, 3(6), 84–100.
29. Zhang, Y.-F., Zhang, N., Hingorani, H., Ding, N., Wang, D., Yuan, C., et al. (2019). Fast-response, stiffness-tunable soft actuator by hybrid multimaterial 3D printing. *Advanced Functional Materials*, 29, 1806698.
30. Kwon, H. J., Osada, Y., & Gong, J. P. (2006). Polyelectrolyte gels-fundamentals and applications. *Polymer Journal*, 38(12), 1211–1219.
31. Koetting, M. C., Peters, J. T., Steichen, S. D., & Peppas, N. A. (2015). Stimulus-responsive hydrogels: Theory, modern advances, and applications. *Materials Science and Engineering: R: Reports*, 93, 1–49.
32. Hou, Y., Chen, C., Liu, K., Tu, Y., Zhang, L., & Li, Y. (2015). Preparation of PVA hydrogel with high transparency and investigations of its transparent mechanism. *RSC Advances*, 5(31), 24023–24030.
33. Gulrez, S. K. H., Al-Assaf, S., & Phillips, G. O. (2011). Hydrogels: Methods of Preparation, Characterisation and Applications. In A. Carpi (Ed.), *Progress in molecular and environmental bioengineering—From analysis and modeling to technology application* (pp. 117–150). London: InTech.
34. Patchan, M., Graham, J. L., Xia, Z., Maranchi, J. P., McCally, R., Schein, O., et al. (2013). Synthesis and properties of regenerated cellulose-based hydrogels with high strength and transparency for potential use as an ocular bandage. *Materials Science and Engineering C*, 33(5), 3069–3076.
35. Vintiloiu, A., & Leroux, J.-C. (2008). Organogels and their use in drug delivery—A review. *Journal of Controlled Release*, 125(3), 179–192.
36. Andrzejewska, E., Marcinkowski, A., & Zgrzeba, A. (2017). Ionogels—Materials containing immobilized ionic liquids. *Polymery*, 62(5), 344–352.
37. Mahadeva, S. K., Kim, J., & Jo, C. (2011). Effect of hydrophobic ionic liquid lading on characteristics and electromechanical performance of cellulose. *International Journal of Precision Engineering and Manufacturing*, 12(1), 47–52.
38. Lee, D., Lee, H., & Jeong, H. (2016). Slurry components in metal chemical mechanical planarization (CMP) process: A review. *International Journal of Precision Engineering and Manufacturing*, 17(12), 1751–1762.
39. Khare, V., Ruby, C., Sonkaria, S., & Taubert, A. (2012). A green and sustainable nanotechnology: Role of ionic liquids. *International Journal of Precision Engineering and Manufacturing*, 13(7), 1207–1213.
40. Kim, J.-H., Shim, B. S., Kim, H. S., Lee, Y.-J., Min, S.-K., Jang, D., et al. (2015). Review of nanocellulose for sustainable future materials. *International Journal of Precision Engineering and Manufacturing-Green Technology*, 2(2), 197–213.
41. Bideau, J., Viau, L., & Vioux, A. (2011). Ionogels, ionic liquid based hybrid materials. *Chemical Society Reviews*, 40(2), 907–925.
42. Willner, I. (2017). Stimuli-controlled hydrogels and their applications. *Accounts of Chemical Research*, 50(4), 657–658.
43. Liem, F., & Urban, M. W. (2010). Recent advances and challenges in designing stimuli-responsive polymers. *Progress in Polymer Science*, 35(1–2), 3–23.
44. Orlov, M., Tokarev, I., Scholl, A., Doran, A., & Minko, S. (2007). pH-responsive thin film membranes from poly(2-vinylpyridine): Water vapor induced formation of a microporous structure. *Macromolecules*, 40(6), 2086–2091.
45. Sannino, A., Demitri, C., & Madaghiale, M. (2009). Biodegradable cellulose-based hydrogels: Design and applications. *Materials*, 2(2), 353–373.
46. Qu, X., Wirsén, A., & Albertsson, A.-C. (2000). Novel pH-sensitive chitosan hydrogels: Swelling behavior and states of water. *Polymer*, 41(12), 4589–4598.
47. Gao, X., Sadasivuni, K. K., Kim, H.-C., Min, S.-K., & Kim, J. (2015). Designing pH-responsive and dielectric hydrogels from cellulose nanocrystals. *Journal of Chemical Sciences*, 127(6), 1119–1125.
48. Way, A. E., Hsu, L., Shanmuganathan, K., Weder, C., & Rowan, S. J. (2012). pH-responsive cellulose nanocrystal gels and nanocomposites. *ACS Macro Letters*, 1(8), 1001–1006.
49. McKee, J. R., Hietala, S., Seitsonen, J., Laine, J., Kontturi, E., & Ikkala, O. (2014). Thermoresponsive nanocellulose hydrogels with tunable mechanical properties. *ACS Macro Letters*, 3(3), 266–270.
50. D’Eramo, L., Chollet, B., Leman, M., Martwong, E., Li, M., Geisler, H., et al. (2018). Microfluidic actuators based on

- temperature-responsive hydrogels. *Microsystems & Nanoeengineering*, 4, 17069–17075.
51. Kim, H., Kim, K., & Lee, S. J. (2017). Nature-inspired thermo-responsive multifunctional membrane adaptively hybridized with PNIPAm and PPy. *NPG Asia Materials*, 9(10), e445–e453.
  52. DeForest, C. A., & Anseth, K. S. (2011). Cyto-compatible click-based hydrogels with dynamically tunable properties through orthogonal photoconjugation and photocleavage reactions. *Nature Chemistry*, 3(12), 925–931.
  53. Takashima, Y., Hatanaka, S., Otsubo, M., Nakahata, M., Kakuta, T., Hashidzume, A., et al. (2012). Expansion–contraction of photoresponsive artificial muscle regulated by host–guest interactions. *Nature Communications*, 3, 1270–1277.
  54. Kim, D., Lee, H. S., & Yoon, J. (2016). Highly bendable bilayer-type photo-actuators comprising of reduced graphene oxide dispersed in hydrogels. *Scientific Reports*, 6, 20921.
  55. Wang, M., Lin, B.-P., & Yang, H. (2016). A plant tendril mimic soft actuator with phototunable bending and chiral twisting motion modes. *Nature Communications*, 7, 13981–13988.
  56. Lee, E., Kim, D., Kim, H., & Yoon, J. (2015). Photothermally driven fast responding photo-actuators fabricated with comb-type hydrogels and magnetite nanoparticles. *Scientific Reports*, 5, 15124–15131.
  57. Zhang, L., Liang, H., Jacob, J., & Naumov, P. (2015). Photogated humidity-driven motility. *Nature Communications*, 6, 7429–7439.
  58. Osada, Y., Okuzaki, H., & Hori, H. (1992). A polymer gel with electrically driven motility. *Nature*, 355(6357), 242–244.
  59. Liang, S., Weng, L., Tan, S., Xu, J., Zhang, X., & Zhang, L. (2007). Field-driven gel actuator with versatile long-range locomotion in air. *Applied Physics Letters*, 90(15), 153506–153508.
  60. Hirai, T., Nemoto, H., Suzuki, T., Hayashi, S., & Hirai, M. (1993). Actuation of poly (vinyl alcohol) gel by electric field. *Journal of Intelligent Material Systems and Structures*, 4(2), 277–279.
  61. Uddin, M. Z., Watanabe, M., Shirai, H., & Hirai, T. (2003). Effects of plasticizers on novel electromechanical actuations with different poly (vinyl chloride) gels. *Journal of Polymer Science Part B: Polymer Physics*, 41(18), 2119–2127.
  62. Liu, G., & Zhao, X. (2006). Electroresponsive behavior of gelatin/alginate semi-interpenetrating polymer network membranes under direct current electric field. *Journal of Macromolecular Science: Pure and Applied Chemistry, Part A*, 43(2), 345–354.
  63. Yang, C., Wang, W., Yao, C., Xie, R., Ju, X.-J., Liu, Z., et al. (2015). Hydrogel walkers with electro-driven motility for cargo transport. *Scientific Reports*, 5, 13622–13631.
  64. Liu, X., He, B., Wang, Z., Tang, H., Su, T., & Wang, Q. (2014). Tough nanocomposite ionogel-based actuator exhibits robust performance. *Scientific Reports*, 4, 6673–6679.
  65. Jayaramudu, T., Li, Y., Ko, H.-U., Shishir, I. R., & Kim, J. (2016). Poly(acrylic acid)-poly(vinyl alcohol) hydrogels for reconfigurable lens actuators. *International Journal of Precision Engineering and Manufacturing-Green Technology*, 3(4), 375–379.
  66. Kim, H. C., Gao, X., Jayaramudu, T., Kang, J., & Kim, J. (2017). Optical and electro-active properties of polyacrylamide/CNC composite hydrogels. *Journal of the Korean Society for Precision Engineering*, 34(8), 575–580.
  67. Wu, Q., Wang, L., Yu, H., Wang, J., & Chen, Z. (2011). Organization of glucose-responsive systems and their properties. *Chemical Reviews*, 111(12), 7855–7875.
  68. Kim, S., & Healy, K. E. (2003). Synthesis and characterization of injectable poly (*N*-isopropylacrylamide-co-acrylic acid) hydrogels with proteolytically degradable cross-links. *Biomacromolecules*, 4(5), 1214–1223.
  69. Zeng, Z., Hoshino, Y., Rodriguez, A., Yoo, H., & Shea, K. J. (2009). Synthetic polymer nanoparticles with antibody-like affinity for a hydrophilic peptide. *ACS Nano*, 4(1), 199–204.
  70. Lu, C., Yang, Y., Wang, J., Fu, R., Zhao, X., Zhao, L., et al. (2018). High-performance graphdiyne-based electrochemical actuators. *Nature Communications*, 9(1), 752–762.
  71. Shahinpoor, M., & Kim, K. J. (2001). Ionic polymer metal composites: I fundamentals. *Smart Materials and Structures*, 10(4), 819–833.
  72. Oguro, K., Kawami, Y., & Takenaka, H. (1992). Bending of an Ion-conducting film-electrode composite by an electric stimulus at low voltage. *Journal of Micromachine Society*, 5, 27–30.
  73. Kim, K. J., & Shahinpoor, M. (2003). Ionic polymer-metal composites: II. Manufacturing techniques. *Smart Materials and Structures*, 12(1), 65–79.
  74. Onishi, K., Sewa, S., Asaka, K., Fujiwara, N., & Oguro, K. (2001). The effects of counter ions on characterization and performance of a solid polymer electrolyte actuator. *Electrochimica Acta*, 46(8), 1233–1241.
  75. Bahramzadeh, Y., & Shehinpoor, M. (2014). A review of ionic polymeric soft actuators and sensors. *Soft Robotics*, 1(1), 38–52.
  76. Oh, I.-K., & Jeon, J.-H. (2015). Ionic polymer-metal composite actuators. In S.-B. Choi & J. Kim (Eds.), *Smart materials actuators: Recent advances in characterization and applications* (pp. 195–212). New York: Nova Science Publishers Inc.
  77. Wang, X. L., Oh, I. K., & Xu, L. (2010). Electro-active artificial muscle based on irradiation-crosslinked sulfonated poly(styrene-ran-ethylene). *Sensors and Actuators B: Chemical*, 145(2), 635–642.
  78. Jo, C., Pugal, D., Oh, I. K., Kim, K. J., & Asaka, K. (2013). Recent Advances in ionic polymer-metal composite actuators and their modeling and applications. *Progress in Polymer Science*, 38(7), 1037–1066.
  79. Cheedarala, R. K., Jeon, J. H., Kee, C. D., & Oh, I. K. (2014). Bio-inspired all-organic soft actuator based on a  $\pi$ - $\pi$  stacked 3D ionic network membrane and ultra-fast solution processing. *Advanced Functional Materials*, 24(38), 6005–6015.
  80. Rajagopalan, M., & Oh, I. K. (2011). Fullereneol-Based electro-active artificial muscles utilizing biocompatible polyetherimide. *ACS Nano*, 5(3), 2248–2256.
  81. Jeon, J. H., Kumar, R., Kee, C. D., & Oh, I. K. (2013). Dry-type artificial muscles based on pendent sulfonated chitosan and functionalized graphene oxide for greatly enhanced ionic interactions and mechanical stiffness. *Advanced Functional Materials*, 23(48), 6007–6018.
  82. Kim, H. J., Randriamahazaka, H., & Oh, I. K. (2014). Highly conductive, capacitive, flexible and soft electrodes based on a 3D graphene-nanotube-palladium hybrid and conducting polymer. *Small (Weinheim an der Bergstrasse, Germany)*, 10(24), 5023–5029.
  83. Fukuda, K., Sekitani, T., Zschieschang, U., Klauk, H., Kuribara, K., Yokota, T., et al. (2011). A 4 V operation, flexible braille display using organic transistors, carbon nanotube actuators, and organic static random-access memory. *Advanced Functional Materials*, 21(21), 4019–4027.
  84. Chae, W., Cha, Y., Peterson, S. D., & Porfiri, M. (2015). Flow measurement and thrust estimation of a vibrating ionic polymer metal composite. *Smart Materials and Structures*, 24(9), 095018–095033.
  85. Shahinpoor, M. (2011). Biomimetic robotic Venus flytrap (*Dionaea muscipula* Ellis) made with ionic polymer metal composites. *Bioinspiration & Biomimetics*, 6(4), 046004–046014.
  86. DeVries, L., Lagor, F. D., Lei, H., Tan, X., & Paley, D. A. (2015). Distributed flow estimation and closed-loop control of an underwater vehicle with a multi-modal artificial lateral line. *Bioinspiration & Biomimetics*, 10(2), 025002–025016.

87. Palmre, V., Pugal, D., Kim, K. J., Leang, K. K., Asaka, K., & Aabloo, A. (2014). Nanothorn electrodes for ionic polymer-metal composite artificial muscles. *Scientific Reports*, *4*, 6176–6185.
88. Wu, G., Hu, Y., Liu, Y., Zhao, J., Chen, X., Whoehling, V., et al. (2015). Graphitic carbon nitride nanosheet electrode-based high-performance ionic actuator. *Nature Communications*, *6*, 7258–7265.
89. Feng, G.-H., & Hou, S.-Y. (2015). Double-section curvature tunable functional actuator with micromachined buckle and grid wire for electricity delivery. *Smart Materials and Structures*, *24*(9), 095010–095022.
90. Kaneto, K. (2016). Research trends of soft actuators based on electroactive polymers and conducting polymers. *Journal of Physics: Conference Series*, *704*(1), 012004–012012.
91. Hara, S., Zama, T., Takashima, W., & Kaneto, K. (2005). Free-standing gel-like polypyrrole actuators doped with bis(perfluoroalkylsulfonyl)imide exhibiting extremely large strain. *Smart Materials and Structures*, *14*(6), 1501–1510.
92. Zama, T., Hara, S., Takashima, W., & Kaneto, K. (2005). Comparison of conducting polymer actuators based on polypyrrole dope with  $\text{BF}_4^-$ ,  $\text{PF}_6^-$ ,  $\text{CF}_3\text{SO}_3^-$ , and  $\text{ClO}_4^-$ . *Bulletin of the Chemical Society of Japan*, *78*(3), 506–511.
93. Madden, J. D., Rinderknecht, D., Anquetil, P. A., & Hunter, I. W. (2007). Creep and cycle life in polypyrrole actuators. *Sensors and Actuators, A: Physical*, *133*(1), 210–217.
94. Otero, T. F., Martinez, J. G., & Arias-Pardilla, J. (2012). Biomimetic electrochemistry from conducting polymers. A Review: artificial muscles, smart membranes, smart drug delivery and computer/neuron interfaces. *Electrochimica Acta*, *84*, 112–128.
95. Takashima, W., Pandey, S. S., & Kaneto, K. (2003). Cyclic voltammetric and electrochemical characteristics of freestanding polypyrrole films in dilute media. *Thin Solid Films*, *438*, 339–345.
96. Pei, Q., & Inganas, O. (1992). Electrochemical applications of the bending beam method. 1. Mass transport and volume changes in polypyrrole during redox. *The Journal of Physical Chemistry*, *96*(25), 10507–10514.
97. Pei, Q., & Inganas, O. (1993). Electrochemical applications of the bending beam method; a novel way to study ion transport in electroactive polymers. *Solid State Ionics*, *60*(1–3), 161–166.
98. Asaka, K., & Okuzaki, H. (2014). *Soft actuators: Materials, modeling, applications, and future perspectives*. New York: Springer Publishing.
99. Daneshvar, E. D., & Smela, E. (2014). Characterization of conjugated polymer actuation under cerebral physiological conditions. *Advanced Healthcare Materials*, *3*(7), 1026–1035.
100. Guimard, N. K., Gomez, N., & Schmidt, C. E. (2007). Conducting polymers in biomedical engineering. *Progress in Polymer Science*, *32*(8–9), 876–921.
101. Lee, K. K., Munce, N. R., Shoa, T., Charron, L. G., Wright, G. A., Madden, J. D., et al. (2009). Fabrication and characterization of laser-micromachined polypyrrole-based artificial muscle actuated catheters. *Sensors and Actuators, A: Physical*, *153*(2), 230–236.
102. Zhou, D., Wallace, G. G., Spinks, G. M., Liu, L., Cowan, R., Saunders, E., et al. (2003). Actuators for the cochlear implant. *Synthetic Metals*, *135*, 39–40.
103. Rogovina, L., Vasil'ev, V. G., & Braudo, E. E. (2008). Definition of the concept of polymer gel. *Polymer Science, Series C*, *50*(1), 85–92.
104. Jager, E. W., Inganas, O., & Lundstrom, I. (2000). Microbots for micrometer-size objects in aqueous media: potential tools for single-cell manipulation. *Science*, *288*(5475), 2335–2338.
105. Tsai, H.-K. A., Moschou, E. A., Daunert, S., Madou, M., & Kulinsky, L. (2009). Integrating biosensors and drug delivery: A step closer toward scalable responsive drug-delivery systems. *Advanced Materials*, *21*(6), 656–660.
106. Berdichevsky, Y., & Lo, Y. H. (2004). Polymer microvalve based on anisotropic expansion of polypyrrole. In D. A. LaVan, A. A. Ayon, M. J. Madou, M. E. McNie, & S. V. Prasad (Eds.), *Micro- and nanosystems* (Vol. 782, pp. 101–107). Warrendale: Materials Research Society.
107. Svennersten, K., Berggren, M., Richter-Dahlfors, A., & Jager, E. W. (2011). Mechanical stimulation of epithelial cells using polypyrrole microactuators. *Lab on a Chip*, *11*(19), 3287–3293.
108. Khaldi, A., Plesse, C., Soyer, C., Cattan, E., Vidal, F., Chevrot, C., et al. (2011). Dry etching process on a conducting interpenetrating polymer network actuator for a flapping fly micro robot. In *ASME 2011 international mechanical engineering congress and exposition, IMECE* (Vol. 2, pp. 755–757).
109. Lu, W., Fadeev, A. G., Qi, B., Smela, E., Mattes, B. R., Ding, J., et al. (2002). Use of ionic liquids for  $\pi$ -conjugated polymer electrochemical devices. *Science*, *297*(5583), 983–987.
110. Baughman, R. H., Cui, C., Zakhidov, A. A., Iqbal, Z., Barisci, J. N., Spinks, G. M., et al. (1999). Carbon nanotube actuators. *Science*, *284*(5418), 1340–1344.
111. Gao, M., Dai, L., Baughman, R. H., Spinks, G. M., & Wallace, G. G. (2000). Electrochemical properties of aligned nanotube arrays: Basis of new electromechanical actuators. *Proc. SPIE 3987, Smart Structures and Materials 2000: Electroactive Polymer Actuators and Devices*. International Society for Optics and Photonics. <https://doi.org/10.1117/12.387798>.
112. Walters, D. A., Ericson, L. M., Casavant, M. J., Liu, J., Colbert, D. T., Smith, K. A., et al. (1999). Elastic strain of freely suspended single-wall carbon nanotube ropes. *Applied Physics Letters*, *74*(25), 3803–3805.
113. Liu, K., Sun, Y., Zhou, R., Zhu, H., Wang, J., Liu, L., et al. (2009). Carbon nanotube yarns with high tensile strength made by a twisting and shrinking method. *Nanotechnology*, *21*(4), 045708–045714.
114. Foroughi, J., Spinks, G. M., Wallace, G. G., Oh, J., Kozlov, M. E., Fang, S., et al. (2011). Torsional carbon nanotube artificial muscles. *Science*, *334*(6055), 494–497.
115. Lima, M. D., Li, N., Andrade, M. J. D., Fang, S., Oh, J., Spinks, G. M., et al. (2012). Electrically, chemically, and photonically powered torsional and tensile actuation of hybrid carbon nanotube yarn muscles. *Science*, *338*(6109), 928–932.
116. Lee, J. A., Kim, Y. T., Spinks, G. M., Suh, D., Lepró, X., Lima, M. D., et al. (2014). All-solid-state carbon nanotube torsional and tensile artificial muscles. *Nano Letters*, *14*(5), 2664–2669.
117. Pelrine, R., Kornbluh, R., Pei, Q., & Joseph, J. (2000). High-speed electrically actuated elastomers with strain greater than 100%. *Science*, *287*(5454), 836–839.
118. Binh, P. C., Nam, D. N. C., & Ahn, K. K. (2015). Design and modeling of an innovative wave energy converter using dielectric electro-active polymers generator. *International Journal of Precision Engineering and Manufacturing*, *16*(8), 1833–1843.
119. Binh, P. C., & Ahn, K. K. (2016). Performance optimization of dielectric electro active polymers in wave energy converter application. *International Journal of Precision Engineering and Manufacturing*, *17*(9), 1175–1185.
120. Carpi, F., Migliore, A., Serra, G., & De Rossi, D. (2005). Helical dielectric elastomer actuators. *Smart Materials and Structures*, *14*(6), 1210–1216.
121. Huang, C., & Zhang, Q. (2004). Enhanced dielectric and electromechanical responses in high dielectric constant all-polymer percolative composites. *Advanced Functional Materials*, *14*(5), 501–506.
122. Bozlar, M., Punckt, C., Korkut, S., Zhu, J., Foo, C. C., Suo, Z., et al. (2012). Dielectric elastomer actuators with elastomeric electrodes. *Applied Physics Letters*, *101*(9), 091907–091911.

123. Kim, J.-Y., Lee, J., Lee, W. H., Kholmanov, I. N., Suk, J. W., Kim, T., et al. (2013). Flexible and transparent dielectric film with a high dielectric constant using chemical vapor deposition-grown graphene interlayer. *ACS Nano*, 8(1), 269–274.
124. Ji, S., Jang, J., Choi, E., Kim, S.-H., Kang, E.-S., Kim, J., et al. (2017). High dielectric performances of flexible and transparent cellulose hybrid films controlled by multidimensional metal nanostructures. *Advanced Materials*, 29(24), 1700538–1700545.
125. Ko, H.-U., Kim, H. C., Kim, J. W., Zhai, L., Jayaramudu, T., & Kim, J. (2017). Fabrication and characterization of cellulose nanocrystal based transparent electroactive polyurethane. *Smart Materials and Structures*, 26(8), 085012–085018.
126. Shi, L., Yang, R., Lu, S., Jia, K., Xiao, C., Lu, T., et al. (2018). Dielectric gels with ultra-high dielectric constant, low elastic modulus, and excellent transparency. *NPG Asia Materials*, 10(8), 821–826.
127. Jayaramudu, T., Ko, H.-U., Zhai, L., Li, Y., & Kim, J. (2017). Preparation and characterization of hydrogels from polyvinyl alcohol and cellulose and their electroactive behavior. *Soft Materials*, 15(1), 64–72.
128. Jayaramudu, T., Ko, H.-U., Kim, H. C., Kim, J. W., Li, Y., & Kim, J. (2017). Transparent and semi-interpenetrating network P(vinyl alcohol)-P(Acrylic acid) hydrogels for electroactive application. *International Journal of Smart and Nano Materials*, 8(2–3), 80–94.
129. Jayaramudu, T., Ko, H.-U., Kim, H. C., Kim, J. W., Muthoka, R. M., & Kim, J. (2018). Electroactive hydrogels made with polyvinyl alcohol/cellulose nanocrystals. *Materials*, 11(9), 1615–1625.
130. Leng, J., Lan, X., Liu, Y., & Du, S. (2011). Shape-memory polymers and their composites: stimulus methods and applications. *Progress in Materials Science*, 56(7), 1077–1135.
131. Hu, J., Zhu, Y., Huang, H., & Lu, J. (2012). Recent advances in shape-memory polymers: Structure, mechanism, functionality, modeling and applications. *Progress in Polymer Science*, 37(12), 1720–1763.
132. Qi, X., Jing, M., Liu, Z., Dong, P., Liu, T., & Fu, Q. (2016). Microfibrillated cellulose reinforced bio-based poly (propylene carbonate) with dual-responsive shape memory properties. *RSC Advances*, 6(9), 7560–7567.
133. Liu, Y., Li, Y., Yang, G., Zheng, X., & Zhou, S. (2015). Multi-stimulus-responsive shape-memory polymer nanocomposite network cross-linked by cellulose nanocrystals. *ACS Applied Materials & Interfaces*, 7(7), 4118–4126.
134. Lu, L., Cao, J., & Li, G. (2018). Giant reversible elongation upon cooling and contraction upon heating for a crosslinked cis poly(1,4-butadiene) system at temperatures below zero Celsius. *Scientific Reports*, 8(1), 14233–14241.
135. Pei, Z., Yang, Y., Chen, Q., Terentjev, E. M., Wei, Y., & Ji, Y. (2014). Mouldable liquid-crystalline elastomer actuators with exchangeable covalent bonds. *Nature Materials*, 13(1), 36–41.
136. Zhao, Q., Zou, W., Luo, Y., & Xie, T. (2016). Shape memory polymer network with thermally distinct elasticity and plasticity. *Science Advances*, 2(1), e1501297–e1501303.
137. Osada, Y., & Matsuda, A. (1995). Shape memory in hydrogels. *Nature*, 376(6537), 219–220.
138. Hu, Z., Zhang, X., & Li, Y. (1995). Synthesis and application of modulated polymer gels. *Science*, 269(5223), 525–527.
139. Kim, H. C., Mun, S., Ko, H.-U., Zhai, L., Kafy, A., & Kim, J. (2016). Renewable smart materials. *Smart Materials and Structures*, 25(7), 073001–073014.
140. Kim, J. (2017). Multifunctional smart biopolymer composites as actuators. In K. K. Sadasivuni, D. Ponnamma, J. Kim, J.-J. Cabibihan, & M. A. Almaadeed (Eds.), *Biopolymer composites in electronics* (pp. 311–331). Amsterdam: Elsevier.
141. Hubbe, M. A., Rojas, O. J., Lucia, L. A., & Sain, M. (2008). Cellulosic nanocomposites: a review. *BioResources*, 3(3), 929–980.
142. Hassan, S. H., Voon, L. H., Velayutham, T. S., Zhai, L., Kim, H. C., & Kim, J. (2018). Review of cellulose smart material: Biomass conversion process and progress on cellulose-based electroactive paper. *Journal of Renewable Materials*, 6(1), 1–25.
143. Kim, J., Yun, S., & Ounaies, Z. (2006). Discovery of cellulose as a smart material. *Macromolecules*, 39(12), 4202–4206.
144. Mahadeva, S. K., Yang, S. Y., & Kim, J. (2011). Electrical and electromechanical properties of cellulose–polypyrrole–ionic liquid nanocomposite: effect of polymerization time. *IEEE Transactions on Nanotechnology*, 10(3), 445–450.
145. Yang, S. Y., Mahadeva, S. K., & Kim, J. (2010). Wirelessly driven electro-active paper actuator made with cellulose–polypyrrole–ionic liquid and dipole rectenna. *Smart Materials and Structures*, 19(10), 105026–105032.
146. Markets, Future. (2018). *The global market for cellulose nanofibers to 2027*. Edinburgh: Future Markets Inc.
147. Mohiuddin, M., Ko, H.-U., Kim, H. C., Kim, J., & Kim, S.-Y. (2015). Transparent and flexible haptic actuator based on cellulose acetate stacked membranes. *International Journal of Precision Engineering and Manufacturing*, 16(7), 1479–1485.
148. Kim, S.-S., & Kee, C.-D. (2014). Electro-active polymer actuator based on PVDF with bacterial cellulose nano-whiskers (BCNW) via electrospinning method. *International Journal of Precision Engineering and Manufacturing*, 15(2), 315–321.
149. Han, M.-W., Song, S.-H., Chu, W.-S., Lee, K.-T., Lee, D., & Ahn, S.-H. (2013). Fabrication of shell actuator using woven type smart soft composite. *Journal of the Korean Society for Precision Engineering*, 30(1), 39–46.

**Publisher's Note** Springer Nature remains neutral with regard to jurisdictional claims in published maps and institutional affiliations.



**Jaehwan Kim** Professor in the Department of Mechanical engineering, Inha University. His research interest is cellulose, smart materials, structure and devices, electroactive polymers and smart sensors.



**Jung Woong Kim** Ph.D. student in the Department of Mechanical engineering, Inha University. His research interest is nanocellulose and composite material.



**Hyun Chan Kim** Postdoctoral researcher in the Department of Mechanical engineering, Inha University. His research interest is nanocellulose, sensor and actuator, microfabrication.



**Hyun-U Ko** Postdoctoral researcher in the Department of Mechanical engineering, Inha University. His research interest is nanocellulose and soft actuators.



**Lindong Zhai** Postdoctoral researcher in the Department of Mechanical engineering, Inha University. His research interest is cellulose EAPap, ACC, nanocellulose, piezoelectric and AFM.



**Ruth M. Muthoka** Ph.D. student in the Department of Mechanical engineering, Inha University. Her research interest is nanocellulose and multifunctional composites.